

Actinometric Assignment of Skin Protection Factor (SPF)  
Values to a Range of Aromatic Alkyl Alkanoates.

by

Tanika Chaisson

A thesis submitted in partial fulfillment  
of the requirements for the degree of  
Bachelor of Science, Honours

Environmental Science, Grenfell Campus  
Memorial University of Newfoundland  
April 2013

© T.Chaisson

Corner Brook

Newfoundland

Grenfell Campus, Memorial University of Newfoundland  
Environmental Science Unit

The undersigned certify that they have read, and recommend to the Environmental Science Unit (Division of Science) for acceptance, a thesis entitled “Actinometric Assignment of Skin Protection Factor (SPF) Values to a Range of Aromatic Alkyl Alkanoates” submitted by Tanika T. Chaisson in partial fulfillment of the requirements for the degree of Bachelor of Science, Honours.

---

Supervisor

April 5, 2013

## **Abstract**

As a result of stratospheric ozone depletion, more ultraviolet (UV) radiation reaches the earth's surface with consequent adverse effects on human health. For this reason, sunscreen product usage has become crucial for sun protection as they absorb the harmful UV radiation. The photoreduction of benzophenone with 2-propanol is a well-known photochemical reaction that has been used for the synthesis of benzpinacol and was used throughout this project with the goal of creating a calibration curve (actinometry) using commercial sunscreens. The parameters of the experiment were optimized to achieve the first point on the curve, but upon testing other sunscreens, insufficient data was collected to create the desired actinometric curve of fractional quantum efficiency versus Sun Protection Factor (SPF) value. For this reason, the calibration curve produced by a similar study by Rolls (2000) was used to deduce the SPF values of methyl salicylate, octyl salicylate, and benzocaine- all common active ingredients in commercial sunscreens- prepared via Fisher Esterification. Octyl salicylate was the only aromatic alkyl alkanoates tested that yielded benzpinacol and the SPF value was found to be 90.

## **Acknowledgments**

First I would like to thank my supervisor, Dr. Julian M. Dust for his support and helpful guidance throughout this honours project. My gratitude goes out as well to all the Environmental Science faculty and technical staff for their advice and support during this experience. Lastly I wish to thank my family and close friends whose enthusiasm and support have helped me achieve this accomplishment.

## Table of Contents

<b>1.0 Introduction</b> .....	1
1.1 Electromagnetic Spectrum of Light.....	1
1.2 Ozone Depletion.....	3
1.3 Effects of Overexposure to UV-B and UV-A.....	3
1.4 Photoprotection.....	5
1.5 Sunscreens.....	6
1.6 Photochemistry.....	9
1.7 Scope of Project. ....	13
<b>2.0 Experimental</b> .....	14
2.1 Materials and Chemicals.. ....	14
2.1.1 Purification of Methanol.....	14
2.1.2 Purification of Ethanol. ....	15
2.1.3 Purification of 1-Octanol.. ....	15
2.1.4 Recrystallization of Benzophenone.....	15
2.2 Preparation of Esters.....	16
2.2.1 Preparation of Methyl Salicylate.....	16
2.2.2 Preparation of Octyl Salicylate .....	17
2.2.3 Preparation of Benzocaine.....	19
2.3 Actinometry.....	20
2.3.1 Optimization of Experimental Parameters.....	20
2.3.2 Actinometric-SPF Calibration Curve Determination.....	22

2.3.3 Estimation of SPF Values for the Ester Sunscreen Components.....	23
<b>3.0 Results &amp; Discussion.....</b>	<b>26</b>
3.1 Esters.....	26
3.1.1 Characterization of Methyl Salicylate.. ..	26
3.1.2 Characterization of Octyl Salicylate. ....	28
3.1.3 Characterization of Benzocaine.....	30
3.2 Actinometry.....	32
3.2.1 Actinometric Assignment of SPF Value to Octyl Salicylate.....	35
3.2.2 Drawbacks in Experimental Design: Photoreduction.....	39
<b>4.0 Conclusion.....</b>	<b>41</b>
4.1 Sun Protection Factor Values.....	41
4.2 Suggestions for Future Work.....	42
<b>References.....</b>	<b>43</b>
<b>Appendix.....</b>	<b>i</b>

## List of Tables

Table 1.1	Structures of common ingredients used in commercial sunscreens.	8
Table 2.1	List of chemicals used and their corresponding supplier and purity.	14
Table 3.1	Characterization of prepared esters.	26
Table 3.2	R <sub>f</sub> values for the Thin Layer Chromatography for unknown crystals from second attempt of preparation of benzpinacol.	33
Table 3.3	Yield of benzpinacol (g) with no sunscreen.	34
Table 3.4	Yield of benzpinacol (g) from octyl salicylate trial.	35
Table 3.5	Comparative yield of benzpinacol (g) for standard reaction (SPF 0) to octyl salicylate.	35
Table 3.6	Comparative molar absorptivity and SPF values for methyl and octyl salicylate	39

## List of Figures

Figure 1.1	The electromagnetic spectrum. The exponential numbers across the top are approximate wavelength values (nm).	2
Figure 1.2.	Eumelanin- a form of the melanin pigment.	6
Figure 1.3	Jablonski diagram.	10
Figure 2.1	Experimental setup for actinometry.	21
Figure 2.2	Platform types in photochemical reactor: platform A holds 3 RB flasks and platform B holds 6 RB flasks.	23
Figure 2.3	Modified experimental setup. Adapted from Rolls, 2000.	25
Figure 3.1	UV-Vis calibration curve for methyl salicylate.	28
Figure 3.2	UV-Vis calibration curve for octyl salicylate.	29
Figure 3.3	UV-Vis calibration curve for benzocaine.	31
Figure 3.4	SPF versus fractional quantum yield calibration curve.	36
Figure 3.5	Typical TLC plate using 40:60 hexane:dichloromethane eluent.	36
Figure 3.6	(A) Relative spectral distribution of halogen bulb (B) Quantity of UV radiation emitted by various sources.	38

## 1.0 Introduction:

The sun is a part of everyday life to which the development and continued existence of life on earth is dependent.<sup>1</sup> Solar radiation irradiates the earth by light photons, reaching both living and non-living matter.<sup>2</sup> The sun warms the earth by its infrared rays, it provides visible light which enables us to see, and also provides energy to primary producers to undergo photosynthesis- the process whereby plants develop and grow to then be utilized as a source of essential human nutrition. The sun can be considered the driving force for most physical, biological, and chemical processes on earth, and is commonly regarded as having beneficial effects.<sup>3,2</sup> However, the ultraviolet (UV) portion of the solar spectrum has introduced problems amongst all the benefits. Although UV radiation accounts for less than 10% of the total solar energy at the earth's surface, it induces excited states in a wide variety of molecules, introducing many acute and chronic sun-damaging consequences to the skin and health of humans.<sup>4,5</sup>

## 1.1 Electromagnetic Spectrum of Light:

The earth is continuously bombarded by a wide range of electromagnetic radiation which emanates from the sun (among other sources) and can be subdivided based on their wavelengths.<sup>6, 7</sup> The electromagnetic spectrum can be categorized according to wavelength and, thus, energy, since the two quantities are inversely proportional to each other (see Figure 1.1).<sup>8</sup> This relationship can be expressed mathematically by Planck's Law (equation 1), where the quantity of energy, E, associated with each photon, is related to frequency (i.e. velocity of light), c, and the wavelength,  $\lambda$  :

$$E = \frac{hc}{\lambda} \quad (\text{eq. 1})$$

From this equation, it can be seen that the shorter the wavelength of light, the greater the energy it transfers to matter when absorbed.<sup>7</sup> Infrared (IR) radiation emitted from the sun is lower in energy, but is crucial for warming the earth. Visible light, with slightly higher energy, generates color by emitting wavelengths detectable by the human eye, but the most environmentally relevant portion of the electromagnetic spectrum is the ultraviolet (UV) region, with wavelengths falling between 50 and 400 nm.<sup>7</sup>

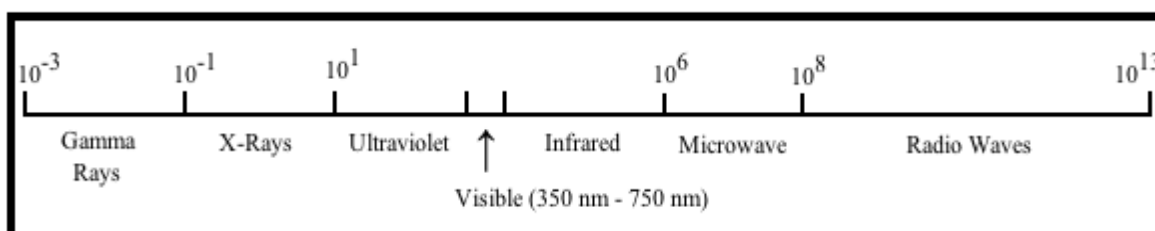


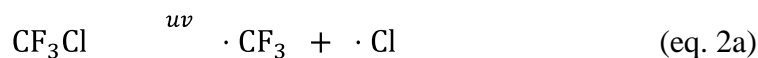
Figure 2.1 The electromagnetic spectrum. The exponential numbers across the top are approximate wavelength values (nm).<sup>8</sup>

UV radiation can be sub-divided into three groups: ultraviolet A (UVA), ultraviolet B (UVB), and ultraviolet C (UVC). The UVC region has the shortest wavelengths of the three groups, ranging between 200-280 nm, and thus possesses the highest energy. The stratospheric ozone layer filters out all of the ultraviolet light in the 220-290 nm range from the sun and, therefore, the high energy UVC rays do not reach the surface of the earth.<sup>7,9</sup> The UVB region lies between 280 and 320 nm, thus the ozone layer is not completely effective in shielding the earth from these rays. This region poses the largest threat to humans biologically because of the high amount of UVB radiation reaching earth and can cause detrimental consequences. The UVA region falls between 320-400 nm and fully penetrates to the surface of the earth, but is the least biologically harmful type of ultraviolet light.<sup>7</sup> All variances aside, the fact that exposure to any type of UV radiation can have consequences is a phenomenon of increasing concern in society.

## 1.2 Ozone Depletion

The ozone layer is an important stratospheric constituent as it absorbs harmful solar ultraviolet light and protects the biosphere, but it is not completely effective in shielding the earth from UVA and UVB light.<sup>4, 7</sup> The quantity of ultraviolet light that strikes the surface of the earth is dependent on several factors, including atmospheric condition, time of day, altitude, latitude and season, but the absorbing capacity of ozone plays the leading role.<sup>9</sup>

As recently as 1980, scientists began accumulating evidence that stratospheric ozone was diminishing in concentration. This problem was primarily caused by the release of anthropogenic chemicals in the atmosphere that have the capability of reacting and enhancing the break-down of ozone.<sup>9</sup> Anthropogenic chlorofluorocarbons (CFCs) can undergo a catalytic sequence that depletes ozone by the following mechanism:<sup>7</sup>



This reduction in ozone concentration allows more UVB radiation from the sun to penetrate to the surface of the earth and has been affecting populated areas in increasing amounts over the past 15 years.<sup>7,9</sup>

## 1.3 Effects of Overexposure to UV-B and UV-A:

Ultraviolet radiation is a natural component of sunlight to which life has evolved and adapted.<sup>4</sup> Today, having a suntan is regarded as a positive thing and can signify an active and healthy lifestyle. UV radiation is also important in vitamin D synthesis- an anticancer agent that is crucial for the body to produce. Vitamin D deficiency can lead to

a reduction in bone growth and regeneration, and increased risk of colorectal and pancreatic cancers, and because approximately 90% of synthesized vitamin D is derived from exposure to sunlight, it is important to introduce UV light into one's daily life.<sup>10</sup> It is with excessive exposure that issues arise and adverse effects are introduced.

The ultraviolet-B light can lead to both acute and long term effects in humans because it can be absorbed by DNA molecules, which can then undergo damaging reactions.<sup>7</sup> One common effect of overexposure to UVB is erythema, which is reddening of the skin resulting from dilation of small blood vessels just below the epidermis, commonly known as "sunburn". UVB is also the critical wavelength to induce carcinogenesis and is the major reason why 90% of the new cancer cases in humans are estimated to result from overexposure to sunlight.<sup>6,7,9</sup>

UVB can also lead to photoaging, which is "characterized by skin changes, such as wrinkles, coarsening, dryness, mottled pigmentation, loss of elasticity, easy bruising, premalignant and malignant growths on sun-exposed areas."<sup>11</sup> Although photoaging is a slow process that takes decades to become apparent, it accounts for 90% of age-associated cosmetic skin defects.<sup>11</sup> Eye damage, such as cataracts, and immunosuppression can also be attributed to UV radiation.<sup>10</sup>

Historically, the harmful impacts of UVB radiation have posed greater concern because of its higher energy, but UVA is also clinically significant.<sup>6</sup> Like UVB, UVA has been associated with increased risk of photoaging, skin cancer, and immunosuppression, but penetrates deeper into the connective tissues of the skin.<sup>6</sup> Detrimental reactive oxygen species (ROS) can be formed in this tissue and can adversely react with lipids, proteins, and DNA, leading to harmful interference with cellular functions.<sup>12</sup>

The severity of these effects is dependent on several factors. Skin types become a variable because each type reacts differently to UV light. In people with fair skin, inflammation and erythema can occur more readily than in individuals with dark skin, who tend to simply tan. Both conditions are signs of UV damage, but skin type has been found to vary with skin cancer risk.<sup>13</sup> Geography and season are other variables that can impact the severity of ultraviolet effects; the radiation of the sun is stronger near the equator and human exposure is more prevalent in the summer.

#### **1.4 Photoprotection:**

In today's society, good health and self-image has become particularly important. The research that has exposed the detrimental effects that ultraviolet sunlight has on the human body has made the development of photoprotection a priority. Several protective measures are recommended by specialists to help minimize the effects of UV radiation.

Public education events are important to notify the public of the need for routine sun protection behavior, and more importantly encouraging young children to be “sun safe” so they continue such habits into adulthood.<sup>10</sup> Behavioral changes such as limiting exposure to UV radiation, especially in the peak period between 10:00 a.m. and 4:00 p.m., and avoiding artificial tanning devices are two simple prevention strategies to reduce photodamage.<sup>9</sup> Depending on the material and color, clothing also has photoprotective properties and therefore clothes, hats, and glasses are recommended when one is exposed to sunlight.<sup>9,10</sup> Recently, orally administered systemic sunscreens have been commercialized, but since 1928, topical sunscreens have played a major role in skin cancer prevention and overall sun protection and are continuing to be developed and advanced.<sup>14</sup>

## 1.5 Sunscreens:

The human body has the ability to absorb UV radiation naturally to ensure it does not initiate any other harmful reactions. The skin contains pigments that are molecules having a combination of double bonds and/or aromatic rings that absorb visible light. The most important pigment of the skin is melanin, which not only gives skin its color, but also has the ability to absorb potentially damaging UVA and UVB radiation.<sup>11</sup>

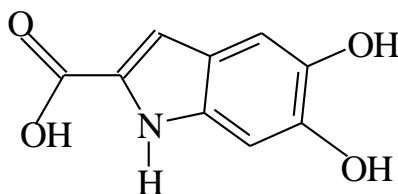


Figure 1.2. Eumelanin- a form of the melanin pigment.<sup>15</sup>

When melanin absorbs the UV radiation, it reduces the risk that the high energy rays will penetrate deeper and react with other chromophores in the body, such as those of deoxyribonucleic acid (DNA), proteins, and lipids, which could result in damaging photobiologic responses.<sup>11</sup>

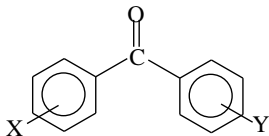
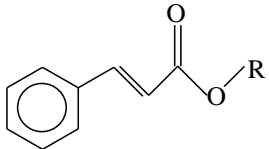
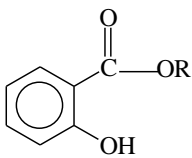
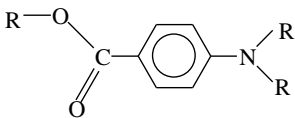
The prevalence of sun damage in humans is increasing; therefore topical sunscreens have been developed with the aim to mimic the function of melanin to reduce potential consequences. After nearly a century since the first commercial sunscreen, there continues to be significant research into sun-protecting agents and many can be purchased in different mediums, including lotions, gels, sprays, and cosmetics. Sunscreens differ in their chemical and physical properties by absorbing, reflecting, or scattering ultraviolet light, but must share the following characteristics:<sup>16,2</sup>

1. Protect against UVA and UVA radiation;
2. Be photostable to avoid formation of ROS;

3. Be user-friendly, reliable, and cost-effective; and
4. Should not penetrate the skin to disrupt DNA cell nuclei.

The first type of topical sunscreen on the market is that which contains physical blocking agents. These are labeled as inorganic filters because they contain inorganic ingredients that act by reflecting or scattering UV solar radiation. The major inorganic agents that are commonly used today are pigment grade nanoparticle powders of metal oxides, specifically zinc oxide (ZnO) and titanium (IV) oxide (TiO<sub>2</sub>) that require a thick application to achieve adequate reflection.<sup>2, 14</sup> The fact that inorganic filters tend to leave an undesired white opaque appearance on the skin increases the popularity of the clear, more convenient chemical blocking agents. Also referred to as organic, chemical filters contain active ingredients that absorb ultraviolet energy at different wavelengths and therefore organic sunscreens can be subcategorized as UVA or UVB filters. These contain anthropogenic chromophores that are responsible for absorbing UV energy, similar to melanin, and converting the absorbed radiation into infrared energy by the radiation-less decay of the molecules that become excited.<sup>2</sup> This conversion occurs when energy from ultraviolet light causes an electron to transform to a higher-energy excited state, and then undergoes a relaxation process to convert the dangerous UV light to harmless energy. Some common organic UVA agents are benzophenones (oxybenzone, sulisobenzone, etc.) and common organic UVB agents include cinnamates, salicylates, and para-aminobenzoic acid (PABA) esters.<sup>14</sup>

Table 4.1 Structures of common ingredients used in commercial sunscreens. <sup>14</sup>

	<b>Ingredient</b>	<b>Structure</b>
UVA blocking agents	Benzophenones	
UVB blocking agents	Cinnamates	
	Salicylates	
	PABA esters	

The effectiveness of a sunscreen in protecting the skin from ultraviolet light damage from the sun is indicated by a sun protection factor (SPF).<sup>11</sup> This technique uses the ratio of the amount of UVB energy required to produce a minimal erythema reaction (MED) through a sunscreen product film to the amount of energy required to produce the same erythema reaction without any sunscreen application (equation 2).<sup>13</sup>

$$\text{SPF} = \frac{\text{MED of sunscreen protected skin}}{\text{MED of non-protected skin}} \quad (\text{eq.3})$$

This is the primary method of evaluating the efficacy of sunscreens, but the validity is somewhat ambiguous since the skin types of test subjects vary and SPF measures the reaction of the skin to erythema- a condition that is 1000 times more likely to occur with UVB radiation versus UVA radiation. For this reason, SPF does not indicate the role that UVA radiation plays in skin cancer, photoaging, or immunosuppression.<sup>6</sup> Another discrepancy in this commonly used technique is that the value placed on the product label is typically less than the true value in an attempt to compensate for the fact that humans rarely apply the recommended standard amount of  $2\text{mg}/\text{cm}^2$ .<sup>13</sup> The controversy about efficiency of SPF and different types of sunscreen suggests that it is important to use a combination of organic and inorganic filters to optimize broad-spectrum photoprotection.<sup>1</sup>

### **1.6 Photochemistry:**

Photochemistry is defined as the chemical reactions and physical processes that may be brought about by the absorption of light.<sup>17</sup> The essential feature of photochemistry is the way that “excited” states of atoms or molecules play a part in the processes and reactions.<sup>17</sup> When these atoms or molecules absorb light, they immediately undergo a change in the organization of their electrons, which is the temporary electronically excited state.<sup>7</sup>

Excited species have the potential to give rise to high energy products such as radicals, biradicals or strained ring compounds which are not readily formed from the ground state. It is these compounds that can potentially react and alter the biological system, resulting in dangerous effects.<sup>18</sup> However; excited states are short-lived and decay back to ground state very rapidly. The excited species must either use the energy to

react photochemically or decay and return to their ground state. The decay processes release energy in a radiative form (fluorescence or phosphorescence) or in a non-radiative form (internal conversion and intersystem crossing).<sup>18</sup> A commonly used diagram to represent all the processes involved in photochemical reactions is the Jablonski diagram, shown in Figure 1.3:

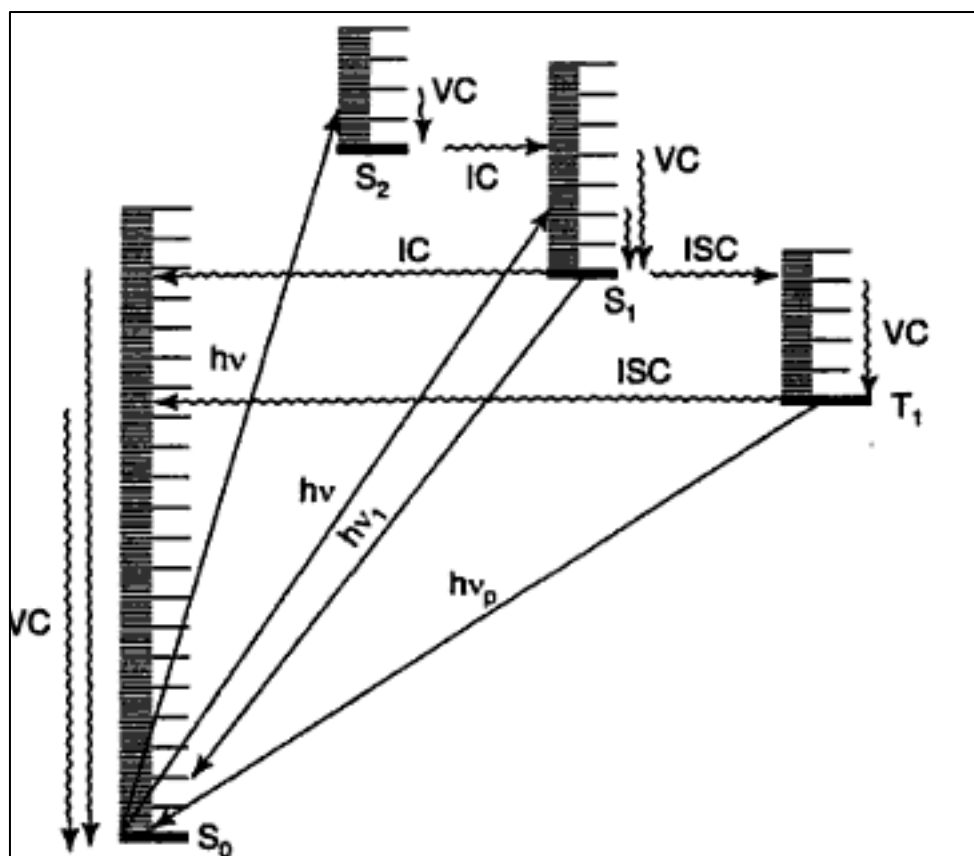


Figure 1.3 Jablonski diagram: IC = Internal Conversion, ISC = Inter-System Crossing,  $h\nu_1$  = Fluorescence,  $h\nu_p$  = Phosphorescence,  $S_0$  = Ground State,  $S_1$  = first single state,  $S_2$  = second single state,  $T_1$  = first triplet state.<sup>19</sup>

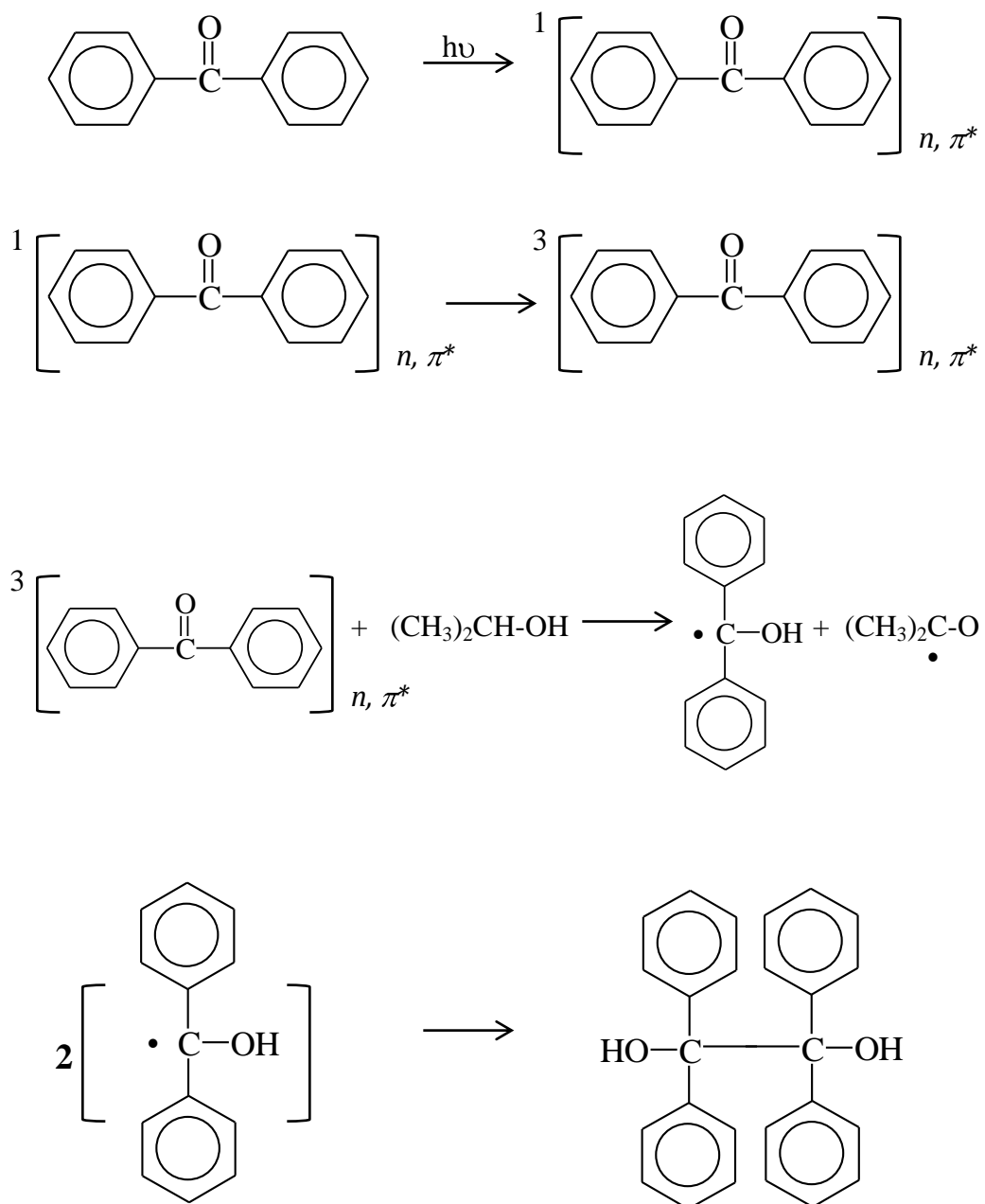
At the beginning of the nineteenth century, the Stark-Einstein law was put forward after the development of the quantum theory and states that if a species absorbs radiation, then one particle is excited for each quantum of radiation absorbed.<sup>17</sup> Since the energy of individual photons are fixed, a higher intensity of light would result in more

photons available for absorption, thus increasing the number of species excited and not an increase of energy available to each individual species.<sup>20</sup> Absorption is a quantum process, therefore the concept of quantum yield was introduced and is defined as the number of molecules of reactant consumed per photon of light absorbed. Quantum yield denotes information about the photochemical behavior and represents the efficiency of the process, thus:<sup>20</sup>

$$\Phi = \frac{\text{rate of reactant disappearance}}{\text{rate of initiation by light}} \quad (\text{eq.4})$$

One of the best understood photochemical reactions is the photoreduction of ketones. Ketones contain two available electronic transitions:  $n - \pi^*$  and  $\pi - \pi^*$ . The  $n - \pi^*$  transition is the lowest energy of the two, therefore the  $S_1$  state will become excited to  $S_2$ , followed by a rapid internal conversion (IC) to the  $^3(n - \pi^*)$  then back down to  $S_1$ .<sup>20</sup> From this state, hydrogen is abstracted from a suitable hydrogen donor to form two radical species. Excited states with the  $\pi - \pi^*$  configuration are less reactive and therefore, less likely to occur.<sup>21</sup> In such photochemical reactions, the excited state energy is lost as heat, and it is this same process that occurs in organic sunscreens. One example of photoreduction is the reaction of a solution of benzophenone in the presence of 2-propanol and UV light, producing benzpinacol and acetone. The efficiency of this photoreduction depends on the nature of the solvent and the ketone, but when 2-propanol is used under suitable conditions, the quantum yield is about 2, which suggests 100% efficiency.<sup>21</sup> This fairly constant quantum yield is a result of the ability of radical produced from the solvent to reduce a molecule of benzophenone to its ketyl radical, and two molecules of benzophenone are removed for each quantum of light absorbed. The

radicals then form the stable dimer product of benzpinacol. The mechanism of this photoreduction is shown below, where the final product is benzpinacol.<sup>21</sup>



The good yields of benzpinacol produced by the sun's ultraviolet light gives consistent quantum yields, therefore this reaction can be used as an actinometer for determining the SPF in the experiment to follow.<sup>17</sup>

### **1.7 Scope of Project:**

The aim of the experimental portion of this research is to estimate the SPF values for selected aromatic alkyl alkanoates. Initially, the reaction of benzophenone and 2-propanol will be used to yield benzpinacol in several different trials using commercial sunscreens with different SPF values. Plotting this data of quantum efficiency (i.e., yield of benzpinacol) versus known SPF values will give a calibration curve, which can then be used to determine the unknown SPF values of the esters tested.

These aromatic alkyl alkanoates will be prepared in the lab using standard techniques, and the purified products will be analyzed by UV-Vis spectroscopy.

## 2.0 Experimental:

### 2.1 Materials and Chemicals

Two esters of salicylic acid and one ester of PABA were all prepared by Fischer Esterification.<sup>22</sup> All starting materials and reagents were obtained commercially and were reagent grade or better. A list of chemicals and their corresponding supplier and purity is outlined in Table 2.1. All reagents were used as purchased, except for methanol, ethanol, 1-octanol, and for one actinometric trial, benzophenone (see 2.1.4). The purification of each is outlined below.

Table 5.1 List of chemicals used and their corresponding supplier and purity.

Chemical	Supplier	Purity
Methanol	Burdick & Jackson	HPLC Grade
Ethanol	Sigma-Aldrich	-
2-propanol	Fisher Scientific	HPLC Grade
1-Octanol	Sigma-Aldrich	99+%
Acetic Acid (Glacial)	Fisher Scientific	ACS Grade
Sulfuric Acid (18M)	Fisher Scientific	ACS Grade
Toluene	Fisher Scientific	HPLC Grade
Diethyl Ether	EMD Millipore	ACS Grade
Ethyl Acetate	Fisher Scientific	HPLC Grade
Dichloromethane	Sigma-Aldrich	-
Acetonitrile	Fisher Scientific	HPLC Grade
Salicylic Acid	ACP Chemicals	99%
Benzophenone	EMD Millipore	-
PABA	Aldrich	99%
Nujol	Alfa Aesar	IR Grade

#### 2.1.1 Purification of Methanol

Removing any water impurities will result in the desired “super” dry methanol. The method used was suggested in Vogel’s Textbook of Practical Organic Chemistry, and utilized a continuous still, cold finger condenser and calcium chloride guard tubes in the drying procedure.<sup>22</sup> A crystal of iodine, 5.10 g of magnesium turnings and 80 mL of

methanol were added to a 1000 mL two-necked round bottom (RB) flask. This solution was refluxed for approximately one hour until the magnesium was converted to magnesium methoxide. After completion of this reaction, an addition 600 mL of methanol was added to the RB flask and refluxed for 40 additional minutes. During this reflux, the magnesium methoxide present in the flask reacted with any excess water with the commercial methanol to produce “super” dry methanol, which was distilled off into a storage vessel.

### **2.1.2 Purification of Ethanol**

To remove excess water in commercial ethanol, the same method was used as outlined above that was suggested by Vogel.<sup>22</sup> A crystal of iodine, 2.55 g of magnesium turnings and 40 mL of ethanol were added to a 1000 mL two-headed RB flask. This solution was refluxed ca. one hour until the magnesium was converted to magnesium ethoxide. After completion of this reaction, an addition 300 mL of methanol was added to the RB flask and refluxed for 40 additional minutes. During this reflux, the magnesium ethoxide present in the flask reacted with any excess water in the commercial ethanol to produce the desired “super” dry ethanol, which was distilled off into a storage vessel.

### **2.1.3 Purification of 1-Octanol**

Octanol was purified by allowing it to stand for one day over four Angstrom (4A, 8-12 Mesh Beads) molecular sieves.

### **2.1.4 Recrystallization of Benzophenone**

In order to maximize the quality of the stock benzophenone, it was purified by recrystallization. The choice of solvent was first determined by testing various solvents

ranging in polarity. The solvents tested included: methanol, 50:50 water: methanol, ethyl acetate, hexane, and toluene. Each of these solvents were added to separate tests tubes containing a small amount of benzophenone and left for five minutes. These tests tubes were then warmed in a hot water bath ca. 10 minutes, and removed from heat and left to cool. From this solvent testing, it was determined that hexane was best suited for recrystallization.

The purification began by obtaining approximately 140 g of stock benzophenone. This was transferred to a 500 mL Erlenmeyer flask and 200 mL of room temperature hexane was added. The flask was placed in a hot water bath and was swirled occasionally; the benzophenone completely entered solution after 45 minutes. The flask was then removed from the heat and allowed to cool to room temperature undisturbed on the lab bench. After approximately 1 hour of cooling, the flask was placed in an ice water bath to maximize crystallization of the benzophenone. The opaque, white diamond-shaped crystals were then collected using vacuum filtration, placed on a watch glass and allowed to dry in the lab overnight.

## **2.2 Preparation of Esters**

### **2.2.1 Preparation of Methyl Salicylate**

Methyl salicylate was prepared by the procedure outlined in a report (ENVS 4950) by Wyn Rolls.<sup>23</sup> The following chemicals were added to a 50 mL RB flask: 5.6 g (0.0405 mol) of salicylic acid, 20 mL (0.4943 mol) of “super” dry methanol, 10 mL of toluene and 1 mL of 18 M sulfuric acid. This RB flask was then attached to a Dean-Stark trap, which contained 25 mL of toluene, and then attached to a condenser. The solution was refluxed for one day, topped up with 40 additional milliliters of dry methanol, then

refluxed for another day. The flask was then disconnected from the condenser and placed on the rotary evaporator for approximately 10 minutes to remove any excess methanol. The solution was cooled and transferred to a separatory funnel with 125 mL of water. After shaking, the upper aqueous layer was discarded and the lower layer was returned to the separatory funnel with a 10% solution of sodium bicarbonate. The purified methyl salicylate layer was then passed through a miniature drying column made from a small Pasteur pipette, cotton, magnesium sulfate and sodium bicarbonate in order to remove any remaining water and/or acid impurities. The yield was 1.24 g (20.1%). Because of this low yield, the procedure outlined above was repeated, but was only refluxed for one day and therefore the additional dry methanol was not required. This second trial resulted in a higher yield of 2.91 g (47.6%).

An infrared spectrum and UV-Vis analysis for methyl salicylate was obtained on the Thermo-Scientific 6700 FTIR Spectrometer and Beckman DU 7400 Spectrophotometer, respectively. The spectra were in good agreement with literature (see section 3.1.1).<sup>24</sup>

### **2.2.2 Preparation of Octyl Salicylate**

Octyl salicylate was prepared using a modified version of the procedure outlined above (2.2.1). The following chemicals were added to a 50 mL RB flask: 5.6 g (0.0405 mol) of salicylic acid, 20 mL (0.1265 mol) of dry 1-octanol, 10 mL of toluene and 1 mL of 18 M sulfuric acid. This RB flask was then attached to a Dean-Stark trap, which contained 25 mL of toluene, and connected to a reflux condenser. The solution was heated to reflux for one day, topped up with 10 additional milliliters of dry 1-octanol, then refluxed for another day. The flask was then removed from the condenser and placed

on the rotary evaporator to remove any excess 1-octanol. Because of the high boiling point of 1-octanol, after 4 hours of rotary evaporation, the alcohol was not entirely removed. In an attempt to properly remove excess 1-octanol, the solution was distilled. After approximately 3 hours of distillation, this procedure resulted in the formation of a black material in the delivering flask; therefore the method was deemed unsuccessful and was terminated.

A second attempt for the preparation of octyl salicylate was modified slightly. The salicylate was chemically prepared using the same proportions of all reagents, except only one drop of 18 M sulfuric acid was used as a catalyst, and 30 mL of 1-octanol was initially used with no further additions. The same techniques were used as outlined above, but after reflux, the octyl salicylate that presumably contained excess 1-octanol was transferred to a 250 mL separatory funnel. This solution was washed with 50 mL of water, where the bottom aqueous layer was discarded, and the organic layer was placed in an Erlenmeyer flask and dried with anhydrous sodium sulfate. This crude product was then filtered through fluted filter paper into an RB flask and the resulting dried organic layer was placed on the rotovap for 2 hours. Since no 1-octanol was collected, vacuum distillation was undertaken using a Welch 1400 duoseal vacuum pump. Under the reduced pressure and heat, octanol distilled off first. This was collected until there was a drastic temperature increase to 105-110°C, and it was at this point that a new receiving flask was attached to the apparatus to allow collection of the purified octyl salicylate. This second attempt yielded 6.88 g (68.2%) of the desired product.

An infrared spectrum and UV-Vis analysis for octyl salicylate was obtained on the Thermo-Scientific 6700 FTIR Spectrometer and Beckman DU 7400 Spectrophotometer, respectively; spectra agreed with literature (see section 3.1.3).<sup>24</sup>

### **2.2.3 Preparation of Benzocaine**

Another esterification was performed to prepare benzocaine from p-aminobenzoic acid (PABA) and used the protocol of the Chemistry 2401 Laboratory Manual published by Sir Wilfred Grenfell College.<sup>25</sup> A mixture of 5 mL of 18 M sulfuric acid with 75 mL of “super” dry ethanol was added to a 125 mL Erlenmeyer and then transferred to a 250 mL RB flask containing 5.00 g of PABA. This was refluxed for approximately 30 minutes (or 10 minutes after the PABA dissolved). A simple distillation was then set up to distill off 50 mL of ethanol into a graduated cylinder, which was stored for later use in recrystallization. After ethanol collection, the RB flask was cooled and poured into a 800 mL beaker. The RB flask was rinsed with 125 mL of deionized water to ensure maximum transfer and this rinse was also transferred to the 800 mL beaker. The solution in the beaker was neutralized with a 2 M sodium carbonate solution that was added cautiously and stirred vigorously. The pH was monitored using pH paper and the addition of base was terminated when the solution was neutral. The beaker was then cooled and the white product was collected in a Buchner funnel using suction filtration. This crude product had a mass of 6.97 g.

The crude product was then dissolved in a minimum amount of recovered ethanol (17 mL) at room temperature in an Erlenmeyer, resulting in an opaque white solution. Activated carbon and an equal amount of water (17 mL) was added to this solution and heated for 2 minutes. This was then filtered through a preheated funnel, where the filtrate

was heated for a second time. After heating, water was added in small portions until the solution just turned cloudy and was then allowed to cool to room temperature. The white crystals were collected in a Buchner funnel using suction filtration and were rinsed with cold water. The crystals were allowed to air dry on a watch glass for 2 days and the final yield was 2.74 g (46.4%).

An infrared spectrum and UV-Vis analysis for benzocaine was obtained on the Thermo-Scientific 6700 FTIR Spectrometer and Beckman DU 7400 Spectrophotometer, respectively. The crystals were also characterized by taking a melting point on the MelTemp II Apparatus, which gave a melting point of 89°C (literature melting point 92°C).<sup>26</sup>

## **2.3 Actinometry**

### **2.3.1 Optimization of Experimental Parameters**

The actinometric chemical system used in this project was the photochemical reaction between 2-propanol and benzophenone to yield benzpinacol. This reaction is known to proceed with quantum yield of unity and was used by Wyn Rolls' report in 2000.<sup>23</sup> Three protocols with modified parameters from method used by Rolls were completed in an attempt to achieve higher benzpinacol yields. Although the first two protocols were deemed unsuccessful, the conclusions and speculative results provoked potential modifications and led to the success of the third protocol.

In the first protocol, a standard run was achieved by preparing three replicates of the reaction. Each replicate was prepared in 100 mL RB flasks containing 9.1 g of benzophenone dissolved in 70 mL of 2-propanol. Nitrogen gas was lightly bubbled through the solution for 30 minutes in order to remove any oxygen present. One drop of

glacial acetic acid was added to the flask while was then filled to the top with 2-propanol and sealed with a rubber septum. The septum was further secured with copper wire and wrapped with parafilm. The three flasks were inverted and placed linearly on a platform inside a box lined with aluminum foil that was arranged under a 60-Watt Full Spectrum lamp (Figure 2.1).

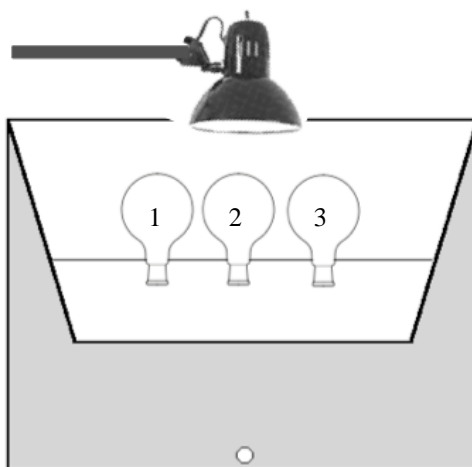


Figure 2.1 Experimental setup for actinometry.

The box setup was covered with aluminum foil to ensure maximum exposure to light, but after 2 hours, it appeared that the heat caused the rubber septa to expand. This resulted in leakage of the solution, so the flasks were topped up with 2-propanol and the foil covering was removed to allow airflow and decrease the chance of overheating. After 12 days of periodic observations, no product was observed, so the three replicates were removed from the apparatus and the solution mixture was discarded.

The same procedure was repeated for the second protocol with one modification: helium gas was used instead of nitrogen gas to bubble through the solutions. After 2 weeks of periodic observations, no product was present in the flasks; therefore the flasks

were removed from the experimental box setup. Instead of discarding the solution, the flasks were left on the bench without exposure to the 60W lamp. After one week on the bench, unidentified elongated crystals were present in the three replicate flasks.

The third protocol used the same principles and proportions of reagents as the methods above, but presented two modifications, one being the switch back to nitrogen gas. Instead of lightly bubbling the nitrogen in solution, it was bubbled vigorously for 30 minutes. Once one drop of glacial acetic acid was added, an addition of 2-propanol was added to almost fill the flask, and the solution was bubbled vigorously for a further 5 minutes. The flask was again topped up with 2-propanol and sealed as before. The second modification used in this protocol was that a 100W halogen bulb was used instead of the 60W full spectrum bulb. After 4 days of being exposed to this new bulb, no crystals appeared, so flask #2 was removed from the setup and placed on the bench for observation. After an additional day, flask #1 and #3 appeared to have a few crystals present in the neck of the flasks. After a total of 12 days of observation, the two flasks remaining in the box setup had significant crystal formation and appeared to cease after 9 days.

### **2.3.2 Actinometric-SPF Calibration Curve Determination**

After a successful trial with the third protocol, the methodology was applied to other trials with the aim to create a calibration curve. The trials employed a similar procedure as above with two modifications: (1) the flasks were bubbled simultaneously, rather than one at a time, and (2) a platform change within the photochemical reactor. The platform previously used could hold three round bottom flasks (Platform A in Figure 2.2) and the modified platform could hold six flasks (Platform B in Figure 2.2). This

difference is presented in Figure 2.2 below. These modifications were put into place in an attempt to minimize preparation time and maximize data output.

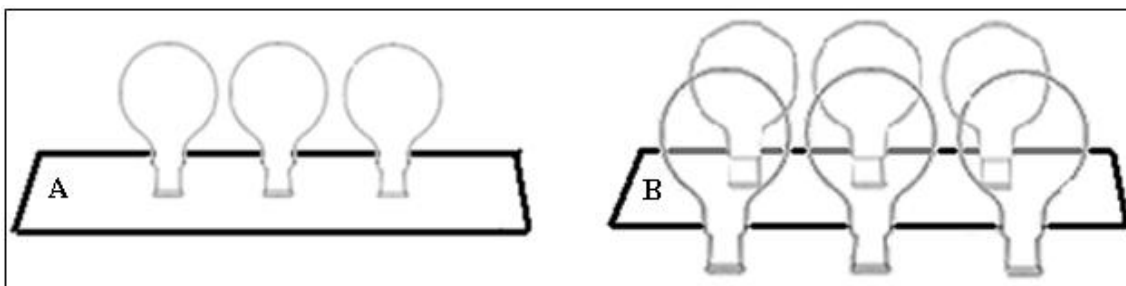


Figure 2.2 Platform types in photochemical reactor: platform A holds 3 RB flasks and platform B holds 6 RB flasks.

In the second semester of this project, additional trials would be completed, where the replicate flasks would be coated with commercial sunscreens with SPF values of 4, 15, 30, 45, 55, and 65 and the benzpinacol yield determined. This wide range of values would add calibration points to the plot previously reported by Rolls.<sup>23</sup> Results are given in Chapter 3.

### 2.3.3 Estimation of SPF Values for the Ester Sunscreen Components

To move forward with this project, two of esters prepared, octyl salicylate and benzocaine, were analyzed in an attempt to deduce their SPF values. The procedure described above was employed again, where three replicate reactions flasks were prepared and bubbled separately for a total of 40 minutes.

Octyl salicylate was tested first by smearing the liquid product over the replicate flasks and placing them in the photochemical reactor. It should be noted that for this trial, the original platform with the capability of holding only three flasks (Platform A in Figure 2.2) was returned to the photochemical reactor to ensure that all conditions were

the same as the only successful trial in which benzpinacol formed. The replicate flasks covered with octyl salicylate were monitored and after 6 days, small crystal formation appeared. These miniscule crystals remained in the flask for 6 additional days and did not show any evidence of growth, therefore the flasks were removed from the photochemical reactor and crystal collection was attempted.

The collection and drying of these crystals was achieved by using sintered glass crucibles with suction filtration. Once the reaction solutions containing the crystals were filtered through the crucible, the product was allowed to dry for approximately 10 minutes. The glass crucibles were weighed before and after the filtration procedure, the difference of weight being indicative of the product yield.

The filtrates from each suction filtration were collected and transferred to 200 mL RB flasks to be rotovapped. It should be noted that the first crucible took significantly longer to filter the reaction solution than the following two, and this led to crystallization of a white product. These crystals were filtered, stored, and the resulting filtrate was treated like the other two filtrates. The first filtrate was placed on the rotary evaporator in hopes of removing the 2-propanol, but after approximately 2 hours of slow evaporation, all the alcohol was still not removed. Due to time constraints, the other two filtrates were not placed on the rotovap but instead, all three RB flasks containing the filtrates were covered with filter paper and placed in the fumehood for 3 days. After this time, the alcohol from the filtrate completely evaporated and a white solid remained in the bottom of the flask. The alcohol from the two other filtrates did not evaporate appreciably, therefore no solid was observed.

Benzocaine was tested next by using the same procedure as outlined for octyl salicylate. The prepared benzocaine was a solid powder; therefore it was mixed with a minimum amount of nujol to enable it to be smeared over the replicate flasks. Upon mixing with the viscous, clear and colorless nujol, the benzocaine was incorporated in the liquid but remained granular and did not dissolve. The replicate flasks covered with the nujol-benzocaine mixture were monitored for 14 days in the photochemical reactor, and then removed from the apparatus due to the absence of product formation.

Due to the lack of results from both trials using the esters, more modifications were endeavored for the final trial of this project to test octyl salicylate for the second time. Recrystallized benzophenone was used in the reaction solution with 2-propanol to ensure maximum purity. The three replicate flasks were prepared in the same manner as previously described, where each were bubbled individually for 35 minutes, then one drop of glacial acetic acid was added and the flasks were topped up with 2-propanol and bubbled for an additional 5 minutes. The original experimental setup shown in Figure 2.1 was retired and the setup that Ms. Rolls used in 2000 was assembled (Figure 2.3).

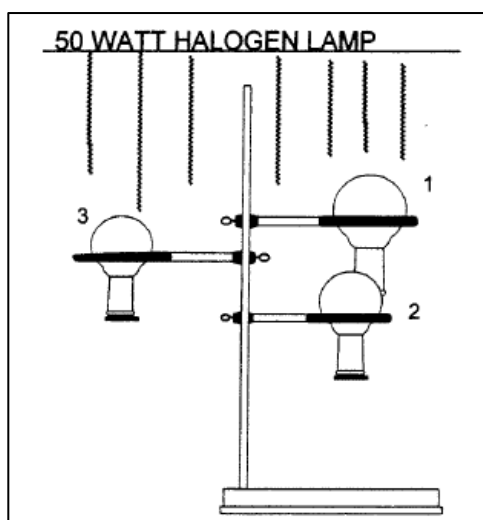


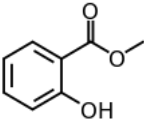
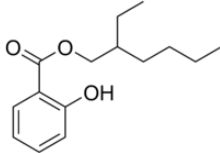
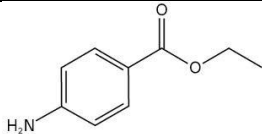
Figure 2.3 Modified experimental setup. Adapted from Rolls, 2000.<sup>23</sup>

### 3.0 Results & Discussion

#### 3.1 Esters

In this project, three esters were prepared: methyl salicylate, octyl salicylate, and benzocaine. The characteristics of these esters are given in Table 3.1 below:

Table 6.1 Characterization of prepared esters.

Compound	Structure	Experimental Melting Point (°C)	Literature Melting Point (°C)	Percent Yield
Methyl Salicylate		-	-	47.6
Octyl Salicylate		-	-	68.2
Benzocaine		89	92 <sup>26</sup>	46.4

##### 3.1.1 Characterization of Methyl Salicylate

The prepared methyl salicylate was characterized by both IR spectrometry and UV-Vis spectrometry. Analysis using the IR spectrometer was achieved by putting a drop of liquid on a NaCl plate, and the resulting IR spectrum is shown in the Appendix (Figure a.1.1). The spectrum showed the expected stretches, including the  $sp^2$  hybridized aromatic C-H stretch at  $3188\text{ cm}^{-1}$ , the  $sp^3$  hybridized aliphatic C-H stretch at  $2955\text{ cm}^{-1}$ , and the intense peak at  $1665\text{ cm}^{-1}$  for the carbonyl group. Other peaks in the fingerprint region were consistent with expected vibrations for methyl salicylate. The experimental

IR spectrum was also compared to one obtained from The National Institute of Standards and Technology (NIST), which can be found in the Appendix (Figure a.1.2), and displayed good correlation.

The UV-Vis spectrum is also found in the Appendix (Figure a.2.1). A value of 1.00 for absorbance and a value of  $10\,000\text{ M}^{-1}\cdot\text{cm}^{-1}$  for the molar absorptivity coefficient ( $\epsilon$ ) were assumed to obtain the concentration needed to optimize the analysis. To calculate this value, the Beer-Lambert Law (equation 4) was used.

$$c = \frac{A}{\epsilon b}, \text{ where } c = \text{concentration} \quad (\text{eq.4})$$

$\epsilon$  = molar absorptivity  
 $b$  = path length (cm)  
 $A$  = absorbance.

The concentration value for methyl salicylate was found to be  $1.0 \times 10^{-4}\text{ M}$ . To prepare this solution, methyl salicylate was dissolved in dichloromethane and serially diluted. When the solution was analyzed, the maximum wavelength was found to be 308.0 nm ( $A = 0.524$ ), and another sharp peak was found to be 244 nm ( $A = 0.684$ ). This was indicative of the benzene ring  $\pi \rightarrow \pi^*$  electronic transition, but the  $n \rightarrow \pi^*$  forbidden transition was not observed on this scale, or was overlapping with the  $\pi \rightarrow \pi^*$  transition, as shown in Figure a.1.1 found in the Appendix. The UV/Vis spectrum was not found for dichloromethane but the approximate wavelength (nm), which the solvent absorbance may be unacceptable in a 1 cm path length, is claimed to be 245 nm by Kaye & Laby Table of Physical & Chemical Constants, 1995.<sup>27</sup> For this reason, the local  $\lambda_{\text{max}}$  at  $\lambda = 244\text{ nm}$  can be assumed to be dichloromethane and therefore is not significant in the determination of molar conductivity of methyl salicylate. Using the absorbance of  $\lambda = 308\text{ nm}$ , the one point epsilon was found to be  $5250\text{ cm}^{-1}\cdot\text{M}^{-1}$ . Using this molar

absorptivity, the concentration of a solution of methyl salicylate to yield a spectrum with an absorbance of 1.00 was calculated. This was then plotted in order to find the experimental molar absorptivity, which was determined to be  $6339 \text{ cm}^{-1} \cdot \text{M}^{-1}$ .

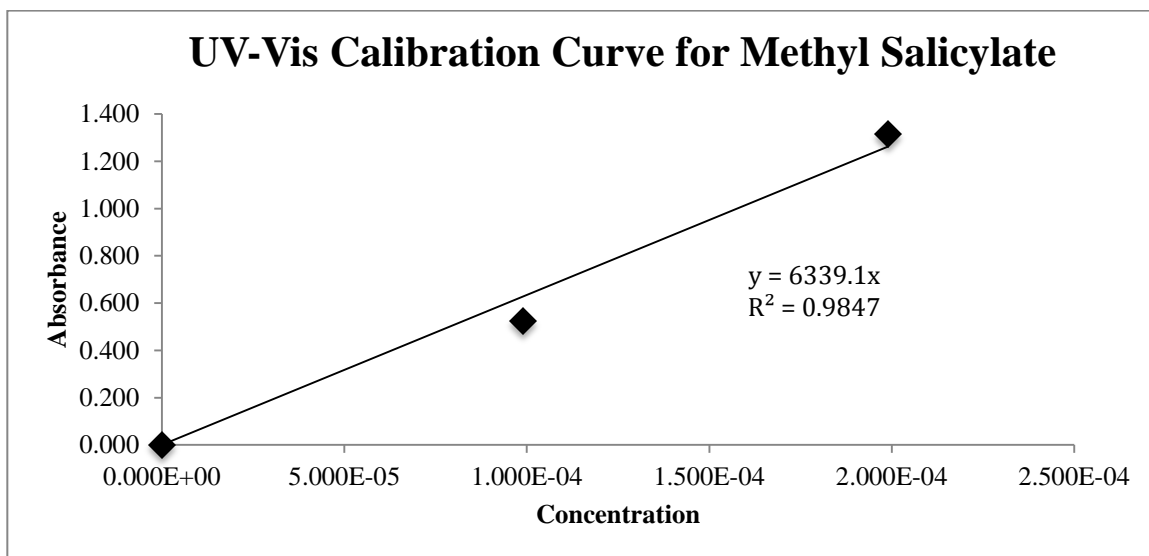


Figure 3.1 UV-Vis calibration curve for methyl salicylate.

### 3.1.2 Characterization of Octyl Salicylate

The prepared octyl salicylate was also characterized by IR spectrometry and UV-Vis spectrometry. Analysis using the IR spectrometer was achieved in the manner by putting a drop of liquid on a NaCl plate, and the resulting IR spectrum is shown in the Appendix (Figure a.1.3). Since octyl salicylate resembles methyl salicylate, the stretches were expected to be similar to the spectrum of the methyl ester. The spectrum showed the expected stretches, similar to methyl salicylate, including the  $sp^2$  hybridized aromatic C-H stretch at  $3184 \text{ cm}^{-1}$ , the  $sp^3$  hybridized aliphatic C-H stretch at  $2956 \text{ cm}^{-1}$ , and the intense peak at  $1671 \text{ cm}^{-1}$  for the carbonyl group. The aliphatic C-H stretching peak was much larger than the same peak in the methyl ester spectrum, but corresponds to the higher amount of carbons in the octyl functional group compared to the methyl group. Other peaks in the fingerprint region were consistent with expected vibrations for octyl

salicylate. The experimental IR spectrum was also compared to one obtained from The National Institute of Standards and Technology (NIST) and displays good correlation.

The UV-Vis spectrum is also found in the Appendix (Figure a.2.2). The same concentration was used to optimize the analysis of octyl salicylate and the solution was prepared also using serial dilution. When the solution was analyzed, the maximum wavelength was found to be 308.0 nm ( $A = 0.374$ ), and another sharp peak was found to

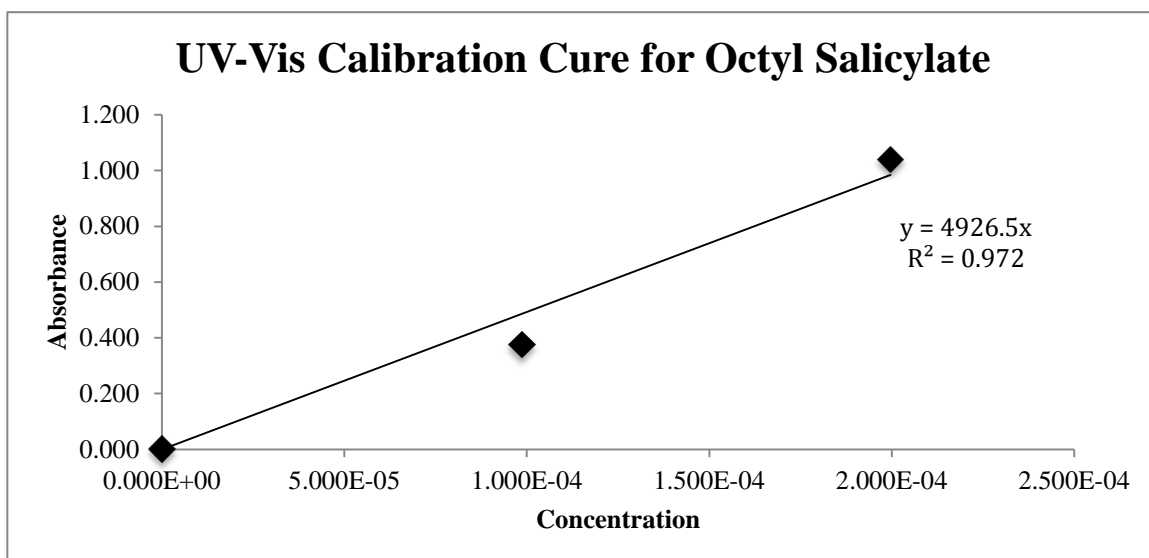


Figure 3.2 UV-Vis calibration curve for octyl salicylate.

be 244 nm ( $A = 0.474$ ). This was indicative of the benzene ring  $\pi \rightarrow \pi^*$  electronic transition, but the  $n \rightarrow \pi^*$  transition was not observed (Figure a.2.2 in the Appendix). The local lambda max at  $\lambda = 244$  nm was again assumed to be dichloromethane, therefore is not significant in the determination of molar conductivity of methyl salicylate. Using the absorbance from  $\lambda = 308$  nm, the one point epsilon was found to be  $3750 \text{ cm}^{-1} \cdot \text{M}^{-1}$ . Using this molar absorptivity, the concentration of a solution of methyl salicylate to yield a spectrum with an absorbance of 1.00 was calculated. This was then plotted in order to find the experimental molar absorptivity, which was determined to be  $4926 \text{ cm}^{-1} \cdot \text{M}^{-1}$ . It is

noteworthy to mention that from the trials performed in this experiment, similar concentrations of both methyl and octyl salicylates were analyzed with UV-Vis spectrometry, and at both concentrations, the absorbance at lambda max was much higher in the methyl salicylate. It can then be speculated that the larger octyl functional group on a salicylate ester will result in less absorbance, thus less efficiency as a sun-protecting chemical when being compared to methyl salicylate.

### **3.1.3 Characterization of Benzocaine**

The prepared benzocaine was also characterized by IR spectrometry and UV-Vis spectrometry. Analysis using the IR spectrometer was achieved by preparing a pellet containing a mixture of 100 mg of KBr and 4 mg of the benzocaine product that was mixed thoroughly and put under high pressure. The benzocaine KBr pellet was then run through the IR spectrometer and the resulting IR spectrum is shown in the Appendix (Figure a.1.4). The spectrum showed the expected stretches, including the N-H amine bonds at  $3422\text{ cm}^{-1}$  and  $3343\text{ cm}^{-1}$ , the  $\text{sp}^2$  hybridized aromatic C-H stretch at  $3045\text{ cm}^{-1}$ , the  $\text{sp}^3$  hybridized aliphatic C-H stretch at  $2984\text{ cm}^{-1}$ , and the peak at  $1682\text{ cm}^{-1}$  for the carbonyl group. The experimental IR spectrum was then compared to the spectra libraries that the instrument had available, and there was an excellent correlation (96%) to benzocaine in KBr found in Georgia State Crime Lab Sample Library, supporting the purity of the product made.

The same technique for UV-Vis spectrometry that was used for the two salicylate esters was applied to benzocaine and the spectrum can be found in the Appendix (Figure a.2.3). Serial dilution was also used to prepare a solution of the determined optimal concentration. When the solution was analyzed, the maximum wavelength was found to be 280.0 nm ( $A = 0.609$ ). This was indicative of the benzene ring  $\pi \rightarrow \pi^*$  electronic transition, but the  $n \rightarrow \pi^*$  transition was not observed (Figure a.2.3 in the Appendix).

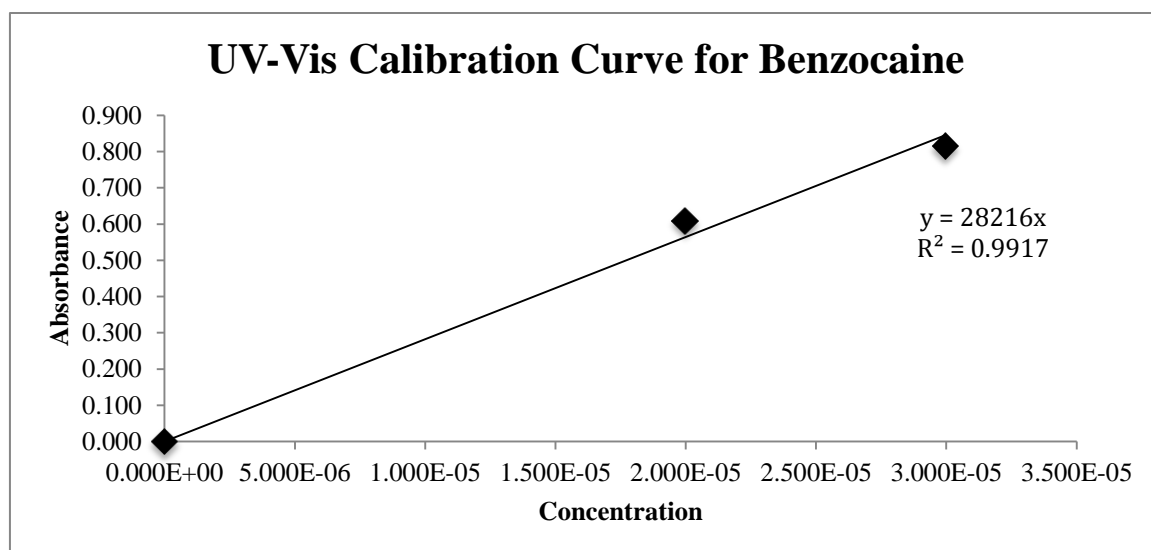


Figure 3.3 UV-Vis calibration curve for benzocaine.

Using the absorbance from  $\lambda = 280$  nm, the one point epsilon was found to be  $30\,500\text{ cm}^{-1}\cdot\text{M}^{-1}$ . Using this molar absorptivity, the concentration of a solution of methyl salicylate to yield a spectrum with an absorbance of 1.00 was calculated. This was then plotted in order to find the experimental molar absorptivity, which was determined to be  $28\,216\text{ cm}^{-1}\cdot\text{M}^{-1}$ .

The final measure taken to characterize benzocaine was to test its melting point. The experimental melting point was  $89^{\circ}\text{C}$  was only a few degrees off from the literature value of  $92^{\circ}\text{C}$  specified by the CRC Handbook of Chemistry and Physics.<sup>26</sup>

### 3.2 Actinometry

The aim of this experiment was to prepare benzpinacol by photolysis using a standard reaction of benzophenone in 2-propanol, which would give a quantum yield of 1. This standard run would then be the starting point of a calibration curve in an attempt to correlate SPF values and quantum yields. In the Fall 2012 semester, three attempts of the standard reaction (SPF 0) with modified parameters from method used by Rolls were completed in an attempt to obtain measurable benzpinacol yields.<sup>23</sup>

The first attempt was unsuccessful. There is a variety of reasons that could account for failure of the photochemical reaction to take place, the first being type of gas used to remove entrained oxygen. Nitrogen gas was used instead of helium gas suggested by Rolls, and was bubbled slowly through the solution.<sup>23</sup> Another reason to account for the absence of reaction could have been the heat that was initially present. Since this forced the rubber septa to expand and leak a small amount of the solution, the reaction solution was altered and may have been contaminated, possibly impacting the photochemical outcome. It is also crucial to note that in this experiment, a full spectrum light bulb was initially used rather than the suggested halogen bulb. This could also have played a role in the absence of product formation due to the variation of light irradiation given off by different light bulbs.

The second attempt that minimized heat was also unsuccessful. Two factors that may have contributed to this failure include inadequate bubbling of helium gas through solution, or an ineffective light source. Helium has a lower molar mass than oxygen, therefore it can be assumed that it would not displace any oxygen that is present from solution as effectively as nitrogen gas, but the fact that it was bubbled slowly could also

have minimized the oxygen removal. It is noteworthy that several days after these reaction flasks were removed from the experimental set up and placed on the bench that crystals formed. In an attempt to determine the identity of the crystals, Thin Layer Chromatography was used to analyze them to determine if the solution still contained the dissolved benzophenone or if there was some benzpinacol present. To achieve this, TLC plates were prepared with a variety of solvent combinations. Two reference chemicals were spotted on the plate: 1. commercial benzophenone dissolved in 2-propanol and; 2. the unknown crystals that were collected from the attempt 2 flasks that were dissolved in dichloromethane. The results are given in Table 3.2.

The polarity variation in the different combinations of solvents could account for the deviations in  $R_f$  values for each solvent, but overall, the  $R_f$  values of the unknown crystals were either the same or very close to the  $R_f$  values for benzophenone. This suggested that no photochemical reaction took place, and the crystals were likely recrystallized benzophenone.

Table 3.2  $R_f$  values for the Thin Layer Chromatography for unknown crystals from second attempt of preparation of benzpinacol.

	<b><math>R_f</math> Values</b>	
<b>Chemical</b>	<b>Trial #1</b>	<b>Trial #2</b>
<b>50:50 diethyl ether:dichloromethane solvent</b>		
Benzophenone	0.84	0.75
Unknown Crystals	0.82	0.75
<b>50:50 ethyl acetate:dichloromethane solvent</b>		
Benzophenone	0.70	0.71
Unknown Crystals	0.81	0.83
<b>50:50 acetonitrile:dichloromethane solvent</b>		
Benzophenone	0.73	0.92
Unknown Crystals	0.86	0.89

In the final attempt, formation of photochemical product was successful. This can be attributed to the vigorous bubbling of nitrogen gas to remove oxygen from the reaction solution, and also the use of the halogen lamp, the same type of lamp suggested by Rolls in 2000.<sup>22</sup> The yield of benzpinacol is shown in Table 3.3.

Table 3.3 Yield of benzpinacol (g) with no sunscreen.

<b>SPF</b>	<b>Flask 1</b>	<b>Flask 3</b>	<b>Average Yield</b>	<b>Quantum Efficiency</b>
0	2.7212	2.5179	2.6196	1

Other calibration points were to be achieved in the Winter 2013 semester by performing the same photochemical reaction for trials with commercial sunscreen layered over the glass RB flasks. For the commercial sunscreen of SPF 4, three replicates of the reaction were prepared in 100 mL RB flasks containing 9.1 g of benzophenone dissolved in 70 mL of 2-propanol. Nitrogen gas was simultaneously bubbled vigorously through the three solutions for 35 minutes, topped up with 2-propanol and one drop of glacial acetic acid was added, then bubbled for an additional 5 minutes. The flasks were then smeared with an even layer of the commercial sunscreen of SPF 4 and placed in the photochemical reactor where they were exposed to the halogen lamp. After 18 days of monitoring the flasks, no product was observed, therefore the three replicates were removed from the apparatus and the solution mixture was discarded.

This procedure was carried out in the same fashion for commercial sunscreens of SPF 30 and 50, where the trials were monitored for approximately two weeks and removed from the photochemical reactor after no product formation was observed. A second trial was attempted for the commercial sunscreen of SPF 30 with a modification addition time of the glacial acetic acid. In this trial, after the 35 minutes of bubbling, the glacial acetic acid was added before the flask was topped up with 2-propanol to ensure

proper mixing of the acid in the reaction solution. After two weeks of monitoring this trial with no product formation, it was established that the modification did not ameliorate the procedure in an attempt to yield crystals. At this point, the testing of commercial sunscreens to collect data to create an improved calibration curve was terminated due to time constraints.

### 3.2.1 Actinometric Assignment of SPF value to Octyl Salicylate

After an unsuccessful attempt to improve upon Rolls' calibration curve prepared in 2000, it was decided that because the benzpinacol yield achieved in the successful trial for bare flasks (SPF 0) was similar to that reported by Rolls, that this calibration curve would be utilized to characterize the SPF values for the successful trial with octyl salicylate.<sup>23</sup> The benzpinacol yields for the octyl salicylate trial is reported in Table 3.4.

Table 3.4 Yield of benzpinacol (g) from octyl salicylate trial.

Crucible	Initial Mass (g)	Final Mass (g)	Yield (g)
1	32.8234	32.8269	0.0035
2	30.8419	30.8561	0.0142
3	30.0577	30.0871	0.0294

The benzpinacol yield from the three replicate flasks varied; therefore the average value was utilized to calculate the quantum efficiency relative to the Rolls data (Table 3.5). It should also be noted that the second trial with octyl salicylate using Rolls' experimental setup (Figure 2.3) did not yield any benzpinacol.

Table 3.5 Comparative yield of benzpinacol (g) for standard reaction (SPF 0) to octyl salicylate.

SPF	Average Yield	Quantum Efficiency
0	2.88095	1
Octyl Salicylate	0.0157	0.0054

Rolls' experimental data demonstrated the linear correlation between SPF and quantum yield of benzpinacol with the following correlation equation:  $SPF = -91.967(\Phi) + 90.901$  (Figure 3.4).<sup>23</sup>

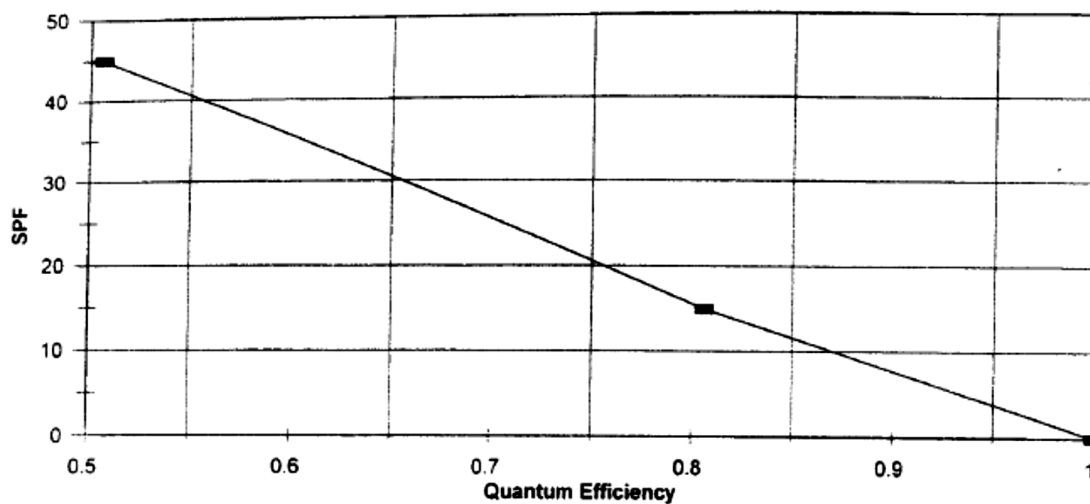


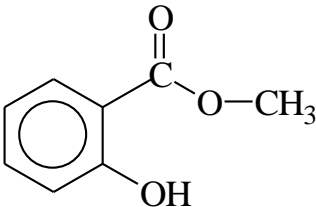
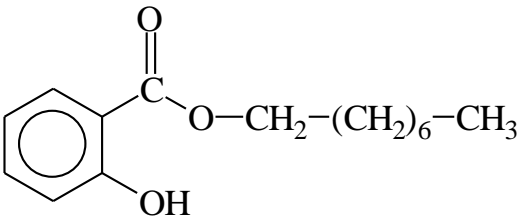
Figure 3.4 SPF versus fractional quantum yield calibration curve. Adapted from Rolls, 2000.<sup>23</sup>

sunscreen tested, assigning a quantum efficiency of 1 for the product yield at SPF 0. The calibration data in Table 3.5 was adapted from Rolls' report in order to estimate the SPF value of the octyl salicylate prepared in this research project, which was determined to be 90.4.<sup>23</sup>

This SPF value for octyl salicylate can also be compared to that of the SPF value of methyl salicylate suggested by Rolls (Table 3.6).<sup>23</sup> The molar absorptivity of methyl salicylate is higher than that of octyl salicylate, suggesting that it would have a higher SPF value, but this is not the case. This inconsistency can be attributed to the volatility of methyl salicylate. During the long period of irradiation, much of the methyl salicylate must have evaporated, whereas the octyl salicylate, with a higher boiling point, remained on the replicate flasks for a longer period of time. It is for this reason that the estimated

SPF value of methyl salicylate was much lower than that of octyl salicylate, and it can be concluded that the latter is the better sun protection compound.

Table 3.6 Comparative molar absorptivity and SPF values for methyl and octyl salicylate.

Compound	Chemical Structure	Molar Absorptivity	SPF Value
Methyl Salicylate		$6339 \text{ cm}^{-1} \cdot \text{M}^{-1}$	12
Octyl Salicylate		$4926 \text{ cm}^{-1} \cdot \text{M}^{-1}$	90

The filtrate that was collected in the successful trial with octyl salicylate was analyzed using Thin Layer Chromatography to determine the identity of its constituents. Four samples were spotted on the TLC plate and included the unidentified filtrate mixture and other standards that were likely components of the filtrates to facilitate comparison.

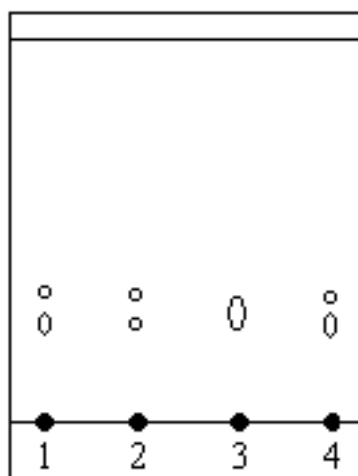


Figure 3.5 Typical TLC plate using 40:60 hexane:dichloromethane eluent.

Figure 3.5 illustrates the location of each spot on the TLC plate, where spot 1 was a sample of stock benzophenone, spot 2 was a sample of benzpinacol that was collected from the successful trial in the Fall 2012, spot 3 was the filtrate from the successful octyl salicylate trial, and spot 4 was first spotted with both benzophenone and benzpinacol. All solid samples were immediately spotted on the TLC plate after being dissolved in dichloromethane. A range of solvent systems was examined (50:50 ethyl acetate: dichloromethane, 50:50 hexane: dichloromethane, hexane, and 40:60 hexane: dichloromethane) and the best eluent was determined to be 40:60 hexane: dichloromethane. Using this eluent, the results from a typical TCL can be seen in Figure 3.5.

The  $R_f$  value for the lower and upper spots for traces 1,2, and 4 were 0.24 and 0.33 respectively. These results suggest that the sample of benzophenone used on spot 1 was not pure, and the sample of benzpinacol used on spot 2 was not pure. Because two compounds were spotted on spot 4, it was expected that two spots would appear on the plate. The  $R_f$  value for spot 3 was also 0.24 but was slightly broader than the other points, suggesting that it contained more than one compound. To further identify these compounds that were present in the filtrate, spot 3 was compared with the other spots. The broad filtrate spot corresponded to an overlap of the spots for benzophenone and benzpinacol, suggesting that the filtrate contained a mixture of both these compounds. These results could agree with the expected incomplete photoreduction of benzophenone to benzpinacol, such that both were still present in the reaction filtrate and thus both appeared to be present through TLC analysis.

### 3.2.2 Drawbacks in Experimental Design: Photoreduction.

The light source used for this part of the research was a 100-Watt halogen bulb. These are considered to be more efficient than incandescent bulbs, but up to 90% of the energy they emit can be in the form of infrared radiation, therefore they operate at a higher temperature.<sup>28, 29</sup> Since the majority of emitted energy lies in the infrared region of the electromagnetic spectrum, the visible and ultraviolet radiation emissions are minimal, falling in the ranges of 15-20% and 1% respectively.<sup>30</sup> The relative spectral distribution of the halogen bulb presented in Figure 3.6 (A) clearly indicates that the majority of the emitted energy are in the infrared region (above 700nm) and that ultraviolet emissions (below 400nm) are minimal. Figure 3.6 (B), which shows the quantity of UV radiation emitted by different sources, indicates the discrepancy of UV emissions between the halogen bulb and sunlight, suggesting that a halogen lamp would poorly mimic the sun.

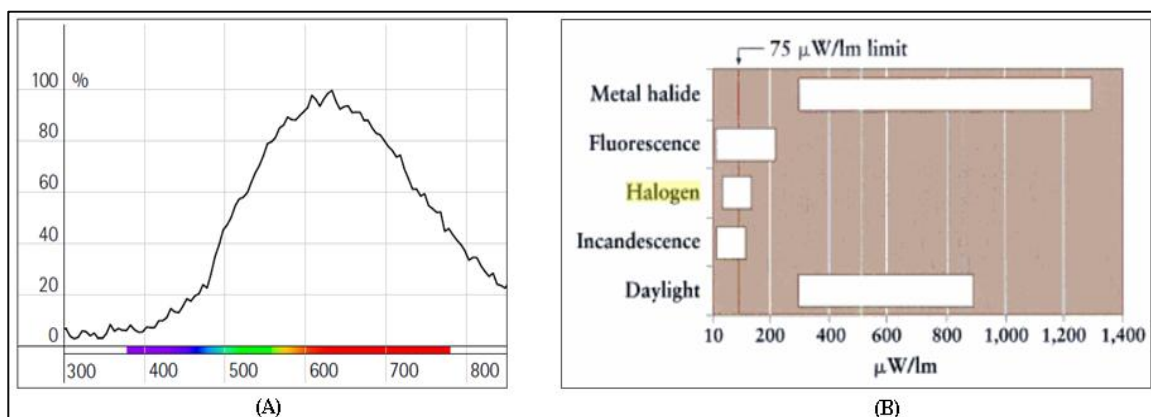


Figure 3.6 (A) Relative spectral distribution of halogen bulb (B) Quantity of UV radiation emitted by various sources.<sup>31, 32</sup>

Another method to rate light bulbs is in terms of luminous efficacy; the efficiency in which electrical power is converted to visible radiation using lumens per watt of electrical power.<sup>30</sup> Energy Star® ranks the halogen bulb as second lowest with a

luminous efficacy of 16-29 lumen/W, surpassing the 12-18 lumen/W efficacy of traditional incandescent bulbs, suggesting that the amount of light radiation emitted is minimal.<sup>29</sup>

The low luminous efficacy and minimal ultraviolet emissions of halogen bulbs are explanations that support why this bulb may not have been ideal for this research project. The photoreduction of the ketone, benzophenone, was utilized to mimic the reaction that would be prevented or minimized by sunscreen ingredients. These sunscreen ingredients are meant to filter ultraviolet radiation from the sun to block it from intersecting with a person's skin; therefore in order for the halogen lamp to effectively mimic the sun's radiation, ultraviolet emissions are required. This could have contributed to the largely unsuccessful photoreduction trials performed throughout this research.

Another source of error in this research experiment to explain the low yields of benzpinacol in the photoreduction of benzophenone was the use of pyrex glass. This type of glass can allow the penetration of lower wavelengths of light energy than that of typical window glass, but does not allow entry of wavelengths below approximately 290 nm. Because UV is light having wavelengths between 50 and 400 nm, the minimal ultraviolet light that actually reached the reaction through the flask may have inhibited the success of the reaction.<sup>33</sup>

## 4.0 Conclusions

### 4.1 SPF Values

The aim of this experiment was achieved throughout eight months of laboratory work. The photochemical reaction between benzophenone and 2-propanol to yield benzpinacol was optimized by testing different parameters in three attempts. It was concluded that vigorous nitrogen bubbling and a 100W halogen lamp are key factors for successful product yields. The third attempt that was deemed successful produced benzpinacol crystals and was considered the standard run, which had no sun protection chemical covering the reaction RB flask (SPF=0). Since the yield achieved in this experiment was similar to that reported by Rolls, it was assumed that upon testing other commercial sunscreens with fixed SPF values, a similar but expanded calibration curve could be created.<sup>23</sup>

Via this calibration curve, Sun Protection Factor (SPF) values of the three aromatic alkyl alkanoates prepared in this project: methyl salicylate, octyl salicylate, and benzocaine. These compounds are reasonable candidates for ingredients in commercial sun protection products and underwent characterization methods including IR and UV-Vis spectrometry, as well as melting points for solids, to confirm their identity and purity. Unfortunately, an ameliorated calibration curve was not achieved because of unsuccessful trials using commercial sunscreens and instead, the calibration curve prepared by Rolls was used to deduce the SPF values of the esters.<sup>23</sup>

The three compounds prepared were applied to RB flasks containing the same proportion of chemicals as the optimal run at SPF 0 and allowed to undergo the expected photochemical reaction. No benzpinacol product was observed for the methyl salicylate

and benzocaine trials; therefore the SPF value could not be deduced. Upon weighing the product yield for octyl salicylate, the quantum yield and SPF value was determined using Rolls' calibration curve and the SPF was found to be very high at a value of 90.<sup>23</sup> Based on this high SPF value, it can be concluded that octyl salicylate would be a good sunscreen ingredient.

#### **4.2 Suggestions for Future Work**

The research results described in this project confirmed that actinometric assignment of SPF values to octyl salicylate could be achieved, and have laid a foundation for continued research. The experimental procedure could be improved so as to give more appropriate yields of benzpinacol crystals by using a light bulb that more effectively mimics sunlight and by using quartz flasks, which would allow more efficient ultraviolet light penetration to reach the reaction solution.

This research could also be repeated for other possible sunscreen ingredients, including cinnamates, benzophenones, and other salicylate esters to estimate their SPF values.

## References

- <sup>1</sup> Diffey, B.L. Sunlight, Skin Cancer and Ozone Depletion. In *Issues in Environmental Science and Technology: Causes and Environmental Implication of Increased UV-B Radiation*; Hester, R.E.; Harrison, R.M., Ed.; The Royal Society of Chemistry: United Kingdom, 2000; Vol. 14; p 107.
- <sup>2</sup> Forestier, S. Rationale for Sunscreen Development. *Journal of the American Academy of Dermatology*. **2008**, 58, S133–8 <http://www.ncbi.nlm.nih.gov/pubmed/18410799>
- <sup>3</sup> Whitehead, R.F.; De Mora, S. Marine Photochemistry and UV Radiation. . In *Issues in Environmental Science and Technology: Causes and Environmental Implication of Increased UV-B Radiation*; Hester, R.E.; Harrison, R.M., Ed.; The Royal Society of Chemistry: United Kingdom, 2000; Vol. 14; p 37.
- <sup>4</sup> Webb, A.R. Ozone Depletion and Changes in Environmental UV-B Radiation. In *Issues in Environmental Science and Technology: Causes and Environmental Implication of Increased UV-B Radiation*; Hester, R.E.; Harrison, R.M., Ed.; The Royal Society of Chemistry: United Kingdom, 2000; Vol. 14; p 19.
- <sup>5</sup> Neale, P.J.; Kieber, D.J. Assessing Biological and Chemical Effects of UV in the Marine Environment: Spectral Weighting Functions. In *Issues in Environmental Science and Technology: Causes and Environmental Implication of Increased UV-B Radiation*; Hester, R.E.; Harrison, R.M., Ed.; The Royal Society of Chemistry: United Kingdom, 2000; Vol. 14; p 67.
- <sup>6</sup> Koshy, J. C.; Sharabi, S. E.; Jerkins, D.; Cox, J.; Cronin, S. P.; Hollier, L. H. Sunscreens: Evolving Aspects of Sun Protection. *Journal of Pediatric Pealth care: Official publication of National Association of Pediatric Nurse Associates & Practitioners*. **2012**, 24(5), 343–6. <http://www.ncbi.nlm.nih.gov/pubmed/20804956>
- <sup>7</sup> Baird, C.; Cann, M. *Environmental Chemistry*, 5<sup>th</sup> ed.; W.H. Freeman and Company: New York, 2012. pp 7-13.
- <sup>8</sup> Kenkel, J. *Analytical Chemistry for Technicians, Third Edition*; CRC Press. 2002. Retrieved from <http://books.google.com/books?id=5aIZ6pO6ljkC&pgis=1>
- <sup>9</sup> Lim, H.; Cooper, K.; Hufford, D.; Ii, T. D.; Trancik, R.; Swerlick, R.; Weinstock, M. A.; Deleo, V., et al. *The Health Impact of Solar Radiation and Prevention Strategies*; Report of the Environment Council, American Academy of Dermatology, 1999, pp 81–99.
- <sup>10</sup> González, S.; Fernández-Lorente, M.; & Gilaberte-Calzada, Y. The Latest on Skin Photoprotection. *Clinics in Dermatology*. **2008**, 26(6), 614–26. <http://www.ncbi.nlm.nih.gov/pubmed/18940542>

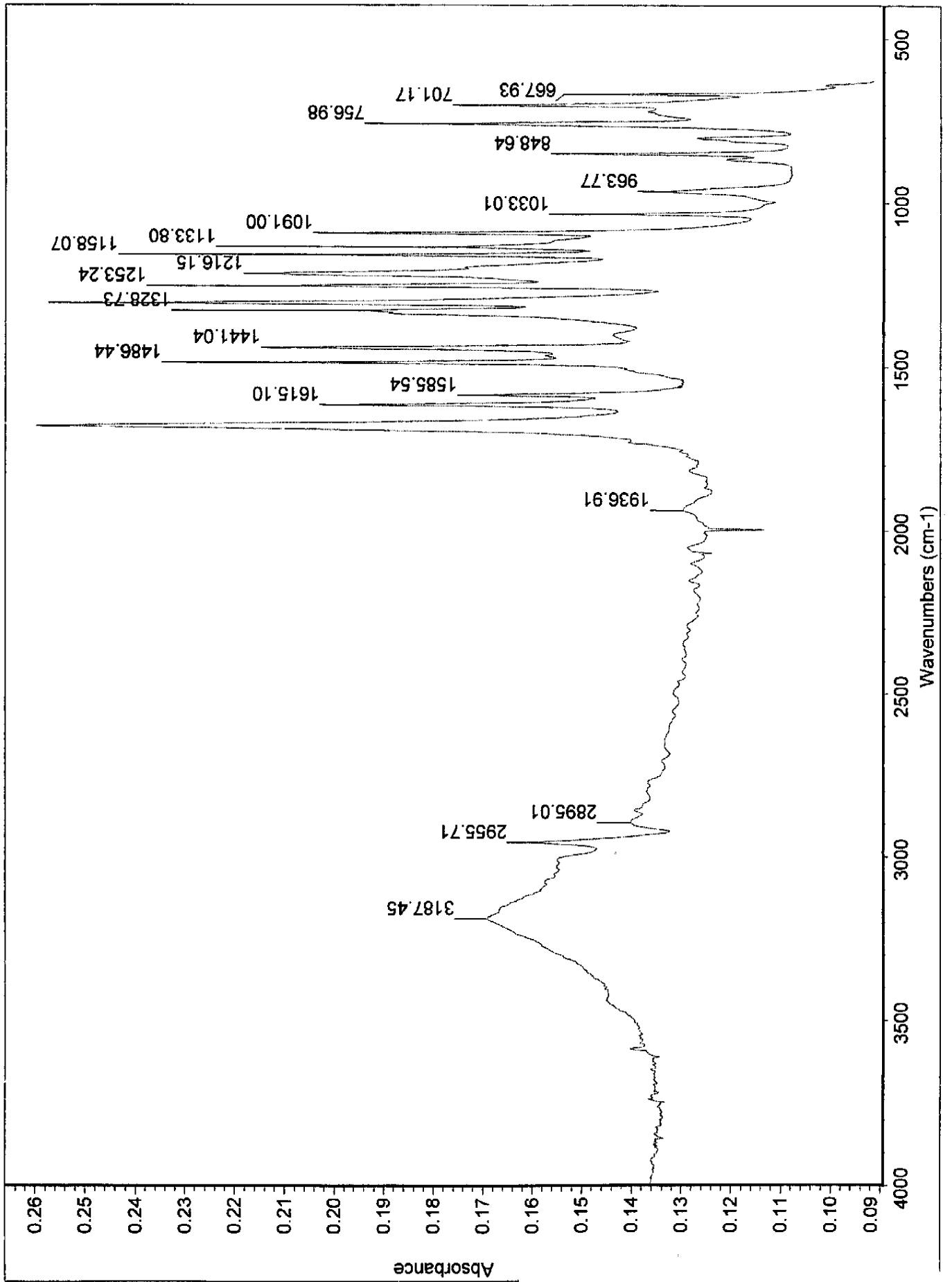
- <sup>11</sup> Guercio-Hauer, C. Photodamage, Photoaging and Photoprotection of Skin. *American Family Physician*. **1994**, 30(2), 327-332.
- <sup>12</sup> Gašperlin, M.; Gosenca, M. Main Approaches for Delivering Antioxidant Vitamins Through the Skin to Prevent Skin Ageing. *Expert opinion on drug delivery*. **2011**, 8(7), 905–19.
- <sup>13</sup> Taylor, C.R.; Stern, R.S.; Leydon, J.J.; Gilchrest, B.A. Photoaging/photodamage and Photoprotection. *Journal of the American Academy of Dermatology*. **1990**, 22, 1.
- <sup>14</sup> Sambandan, D. R.; Ratner, D. Sunscreens: An Overview and Update. *Journal of the American Academy of Dermatology*. **2011**, 64(4), 748–58.  
<http://www.ncbi.nlm.nih.gov/pubmed/21292345>
- <sup>15</sup> Watt, E.R.; Bothma, J.P.; Meredith, P. The Supramolecular Structure of Melanin. *Soft Matter*. **2009**, 5, 3754-3760.  
<http://pubs.rsc.org/en/content/articlepdf/2009/sm/b902507c>
- <sup>16</sup> Serpone, N.; Dondi, D.; Albini, A. Inorganic and Organic UV filters: Their Role and Efficacy in Sunscreens and Suncare Products. *Inorganica Chimica Acta*. **2007**, 360(3), 794–802.  
<http://www.sciencedirect.com/science/article/pii/S0020169306000259>
- <sup>17</sup> Wayne, R.P. *Principles and Applications of Photochemistry*; Oxford Science Publications: New York, 1988. pp 1-2, 144.
- <sup>18</sup> Barltrop, J.A.; Coyle, J.D. *Principles of photochemistry*; John Wiley and Sons: Chichester, 1978. pp 2, 9-10.
- <sup>19</sup> Singh, J. *Photochemistry And Pericyclic Reactions*; New Age International. 2005. p 400. <http://books.google.com/books?id=tnKRNgdzbXMC&pgis=1>
- <sup>20</sup> Wayne, C.E.; Wayne, R.P. *Photochemistry*. Oxford University Press: New York, 1996. pp 2, 10.
- <sup>21</sup> DePuy, C.H.; Chapman, O.L. *Molecular Reactions and Photochemistry*. Prentice-Hall Inc.: New Jersey, 1972. pp 44-49
- <sup>22</sup> Vogel, A.I. *Vogel's Textbook of Practical Organic Chemistry*, 5<sup>th</sup> Edition; Longman Group Inc.: United Kingdom, 1989. pp 401, 1078
- <sup>23</sup> Rolls, Wyn. The Correlation of Actinometry and Skin Protection Factor (SPF). The Estimation of the SPF of a Sun Screen Chemical: Methyl Salicylate. Environmental Science 4950 Project Report, Sir Wilfred Grenfell College, Corner Brook, NL, 2000.

- <sup>24</sup> P.J. Linstrom and W.G. Mallard, Eds., **NIST Chemistry WebBook, NIST Standard Reference Database Number 69**, National Institute of Standards and Technology, Gaithersburg MD, 20899, <http://webbook.nist.gov>, (retrieved December 4, 2012).
- <sup>25</sup> *Chemistry 2401 Introductory Organic Chemistry II Laboratory Manual*; Sir Wilfred Grenfell College: Corner Brook, NL, 2011; p 35-36.
- <sup>26</sup> Lide, D.R. *CRC Handbook of Chemistry and Physics*, 90<sup>th</sup> Edition; CRC Press: New York, 2009/2012. pp 3-233, 3-236, 4-39, 4-92.
- <sup>27</sup> Tables of Physical & Chemical Constants (16<sup>th</sup> edition 1995). 2.1.4 Hygrometry. Kaye & Laby Online. Version 1.0 (2005) [www.kayelaby.npl.co.uk](http://www.kayelaby.npl.co.uk)
- <sup>28</sup> General Electric Lighting North America. FAQ's: Commercial Lighting Information. <http://www.gelighting.com/LightingWeb/na/resources/faqs/> (accessed March 12, 2013).
- <sup>29</sup> Energy Star®. Lighting Technologies: A Guide To Energy-Efficient Illumination. [http://www.energystar.gov/ia/partners/promotions/change\\_light/downloads/Fact%20Sheet\\_Lighting%20Technologies.pdf?0a6b-dfcf](http://www.energystar.gov/ia/partners/promotions/change_light/downloads/Fact%20Sheet_Lighting%20Technologies.pdf?0a6b-dfcf) (accessed March 12, 2013).
- <sup>30</sup> Davidson, M.W. ZEISS Microscopy Online Campus: Tungsten-Halogen Lamps. <http://zeiss-campus.magnet.fsu.edu/articles/lightsources/tungstenhalogen.html> (accessed March 12, 2013).
- <sup>31</sup> ERCO. Guide: Lighting Technology. [http://www.erco.com/download/data/30\\_media/25\\_guide\\_pdf/120\\_en/en\\_erco\\_guide\\_6\\_lighting\\_technology.pdf](http://www.erco.com/download/data/30_media/25_guide_pdf/120_en/en_erco_guide_6_lighting_technology.pdf) (accessed March 12, 2013).
- <sup>32</sup> Lavedrine, B. A Guide to the Preventative Conservation of Photograph Collections. Lavedrine, B.; Gandolfo, J.P., Ed.; Getty Publications: California, 2003; p 155.
- <sup>33</sup> PYREX®. Glass Code 7740: Material Properties. [http://www.glassfab.com/file/sites%7C\\*%7C537%7C\\*%7CDataSheets%7C\\*%7Corning-Pyrex.pdf](http://www.glassfab.com/file/sites%7C*%7C537%7C*%7CDataSheets%7C*%7Corning-Pyrex.pdf) (accessed March 12, 2013).

## Appendix

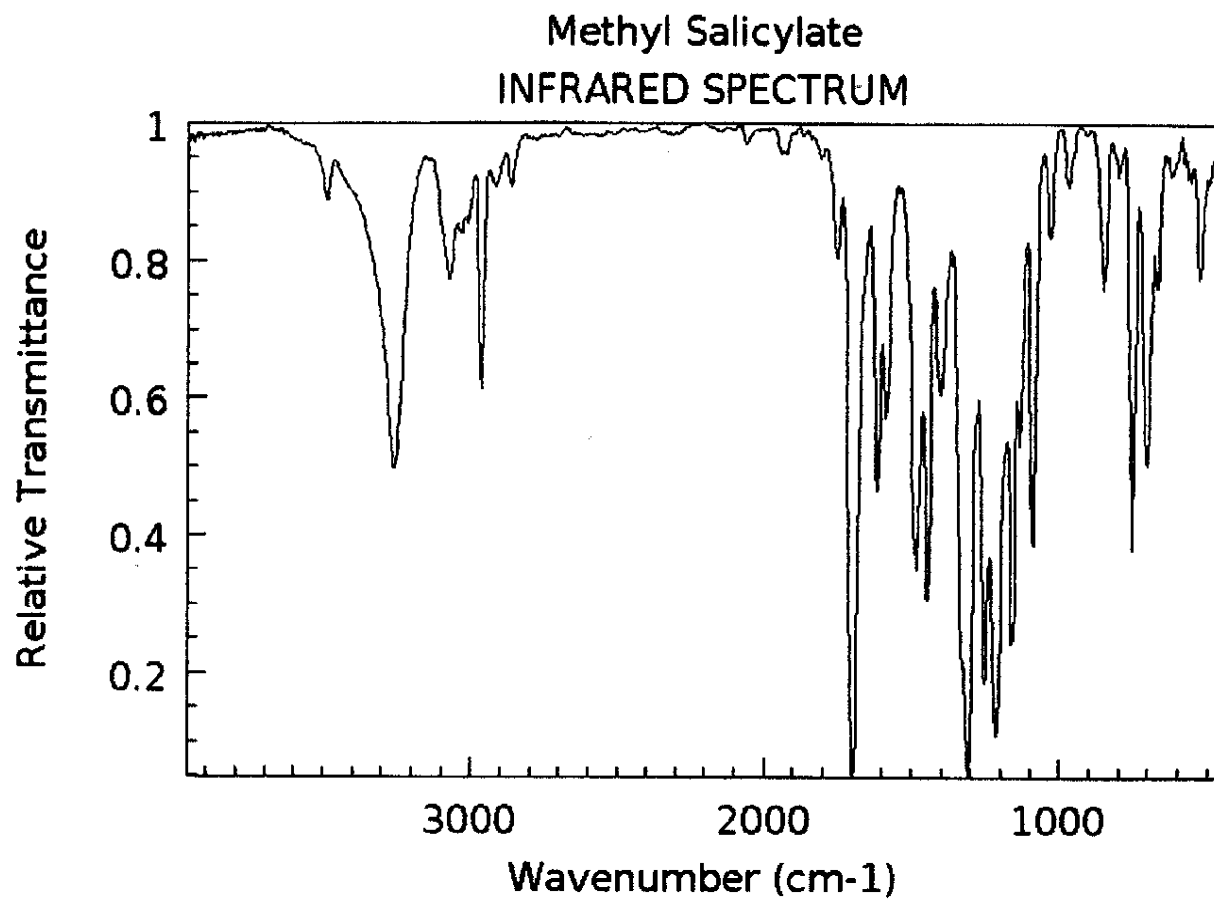
•  
•  
•  
•  
•  
•  
•

•



1. Infrared spectroscopy for methyl salicylate.

Figure a.1.2 NIST IR Spectrum for methyl salicylate.



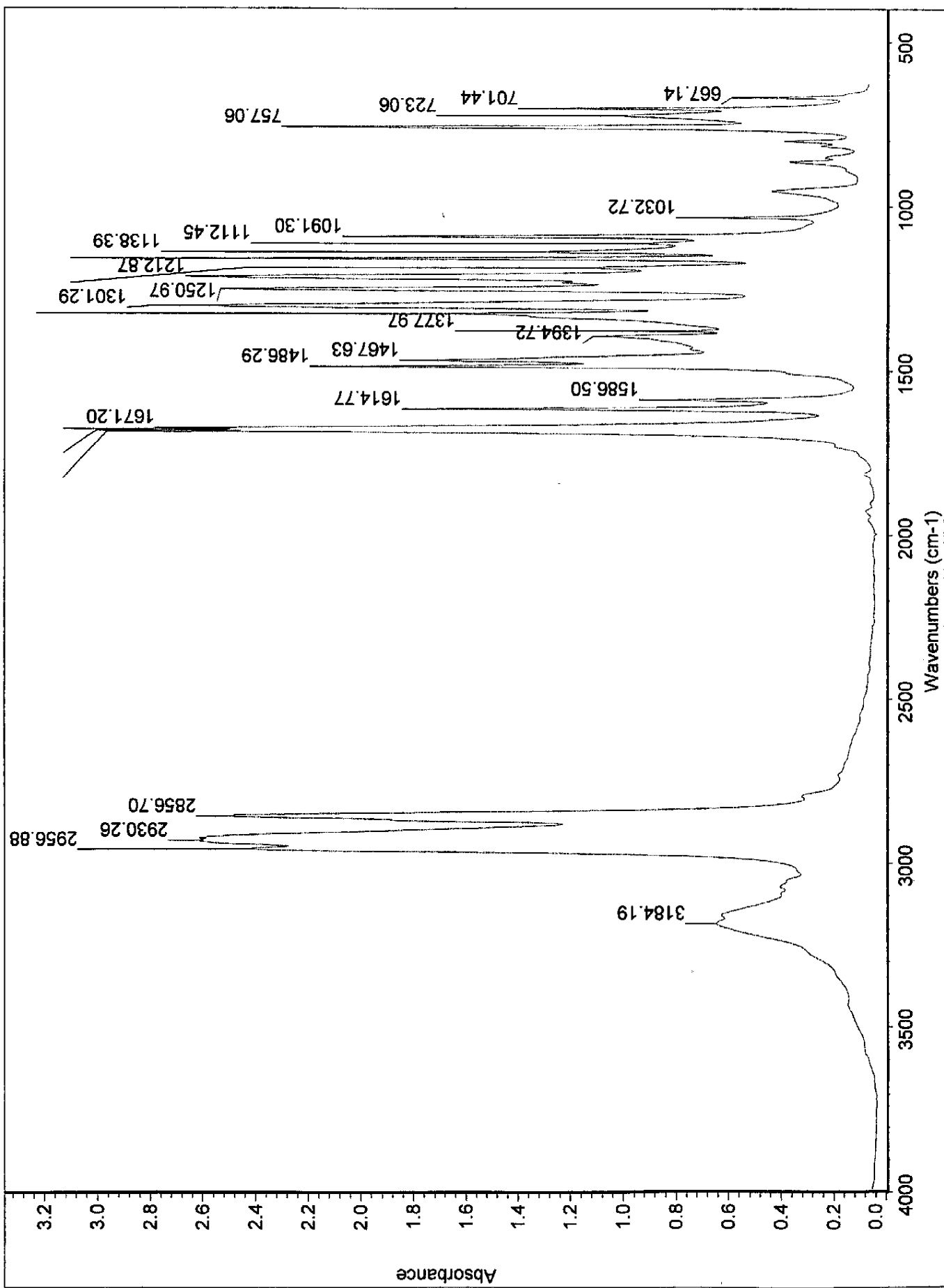
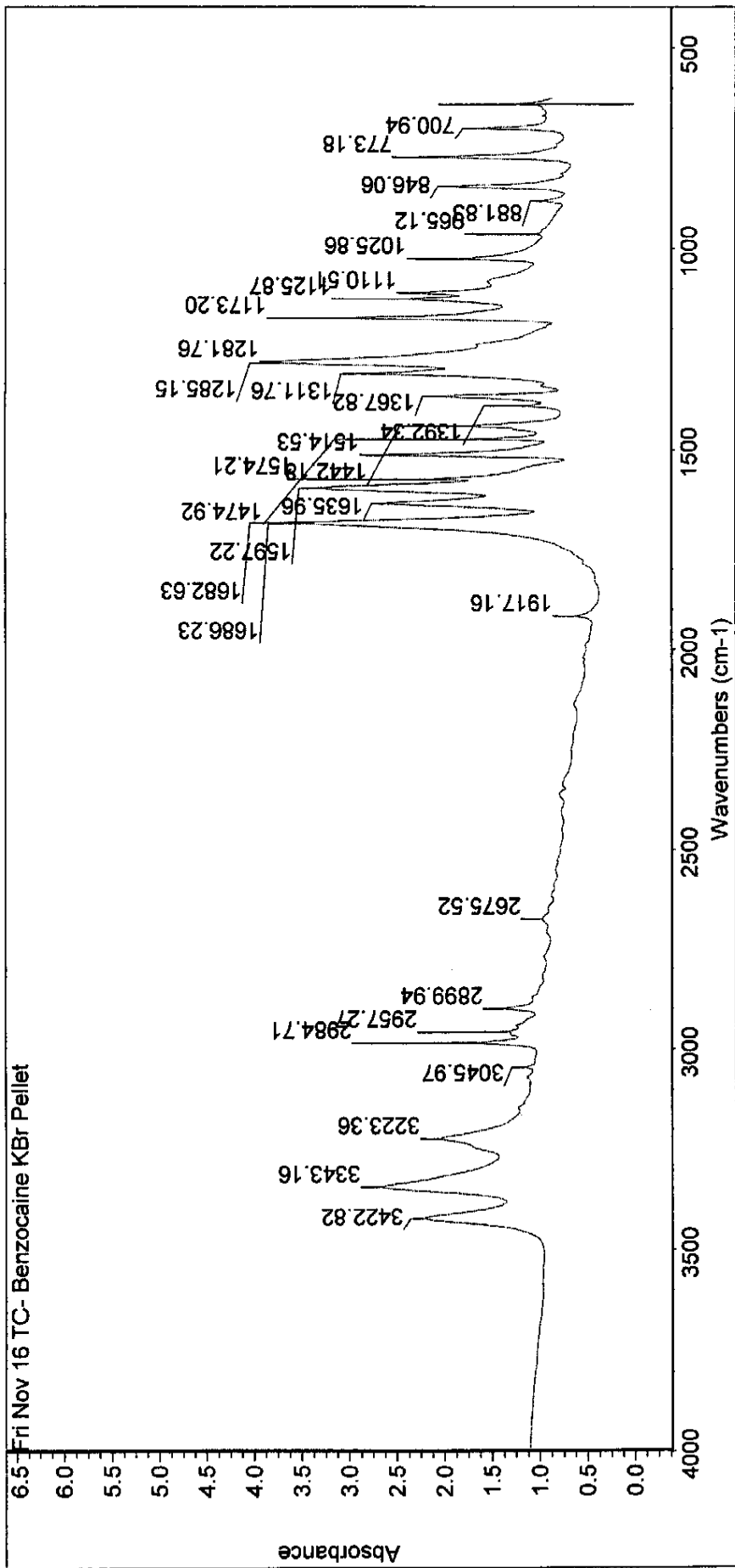


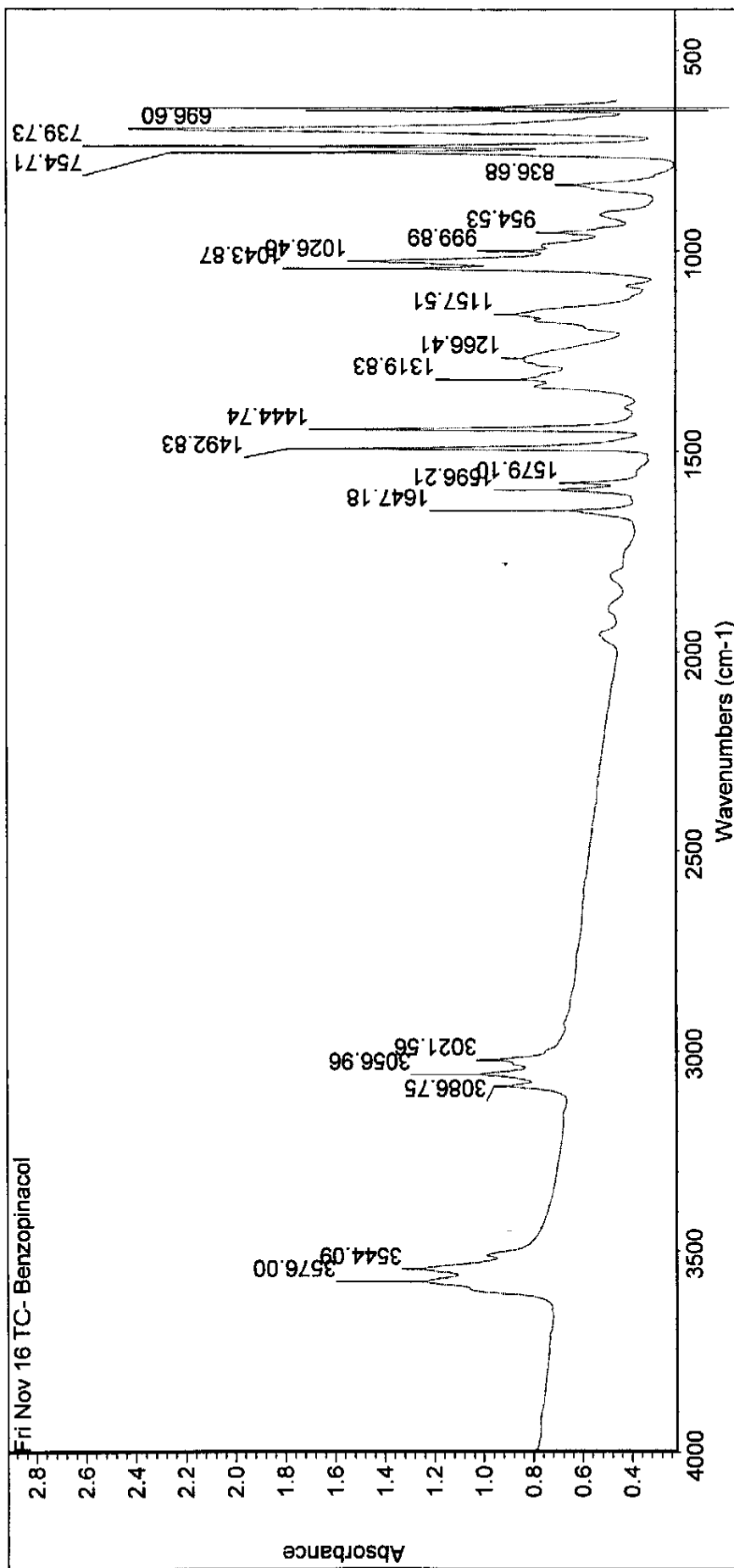
Figure a.1.3 IR Spectrum for octyl salicylate. In good agreement with NIST Webbook.



Fri Nov 16 12:59:06 2012 (GMT-03:30)  
**FIND PEAKS:**  
 Spectrum: Fri Nov 16 TC- Benzocaine KBr Pellet  
 Region: 4000.00 400.00  
 Absolute threshold: 0.560  
 Sensitivity: 50  
 Peak list:

Position:	Intensity:
639.89	1.233
700.94	1.652
773.18	2.313
846.06	1.908
881.83	0.935
965.12	1.023
1025.86	1.780
1110.51	2.257

Figure a.1.4 IR Spectrum for benzocaine. In good agreement with the literature.



Fri Nov 16 12:06:52 2012 (GMT-03:30)

FIND PEAKS:

Spectrum: Fri Nov 16 TC- Benzopinacol

Region: 4000.00 400.00

Absolute threshold: 0.549

Sensitivity: 50

Peak list:

Position:	Intensity:
644.37	1.389
651.64	1.061
696.60	2.416
739.73	1.729
754.71	1.554
836.68	0.611
954.53	0.690
999.89	0.824

Figure a.1.5 IR Spectrum for benzopinacol. In good agreement with the literature.

## II. Ultraviolet-visible spectroscopy

Figure a.2.1 UV-Vis Spectrum for methyl salicylate.

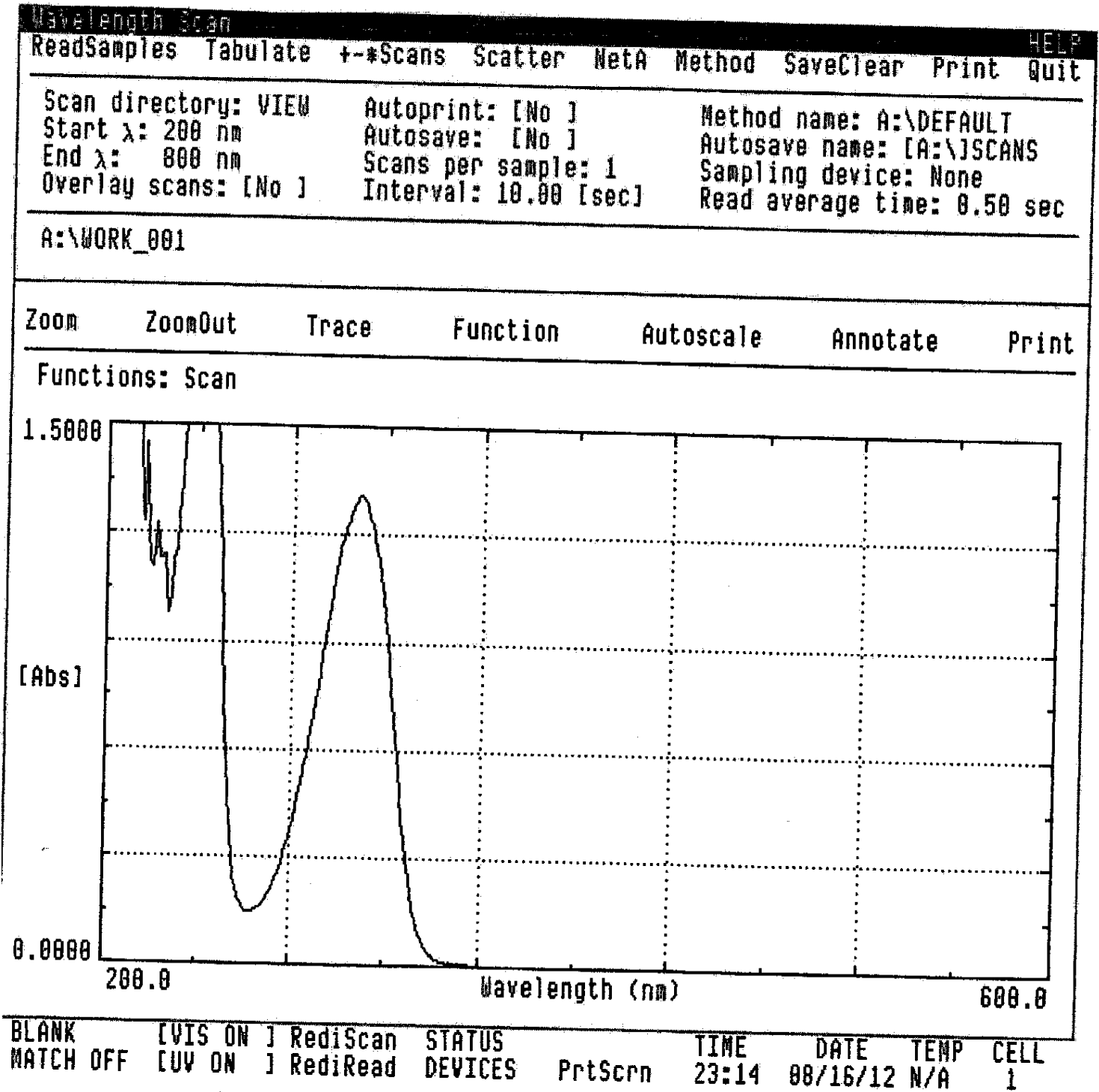


Figure a.2.2 UV-Vis Spectrum for octyl salicylate.

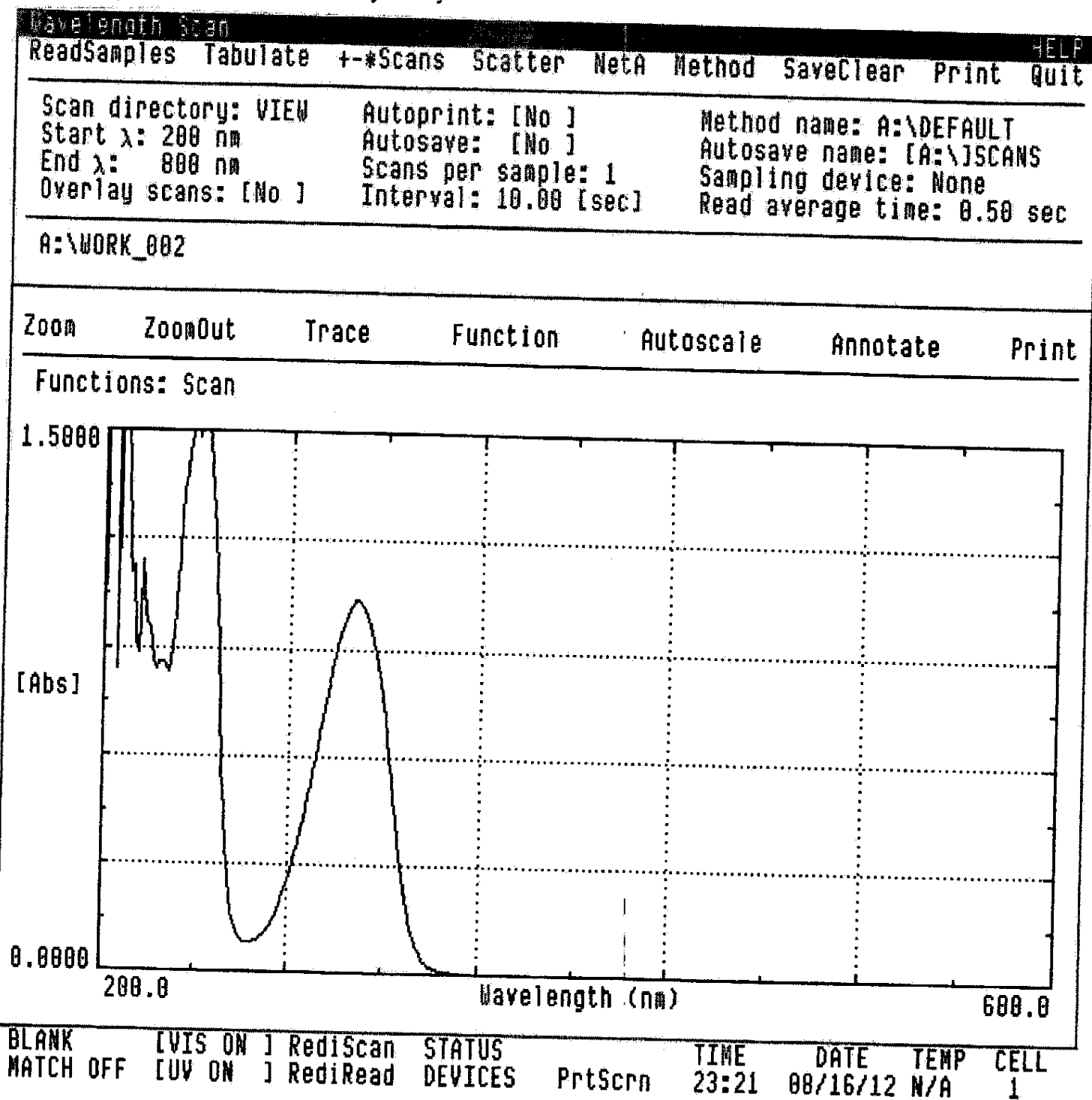
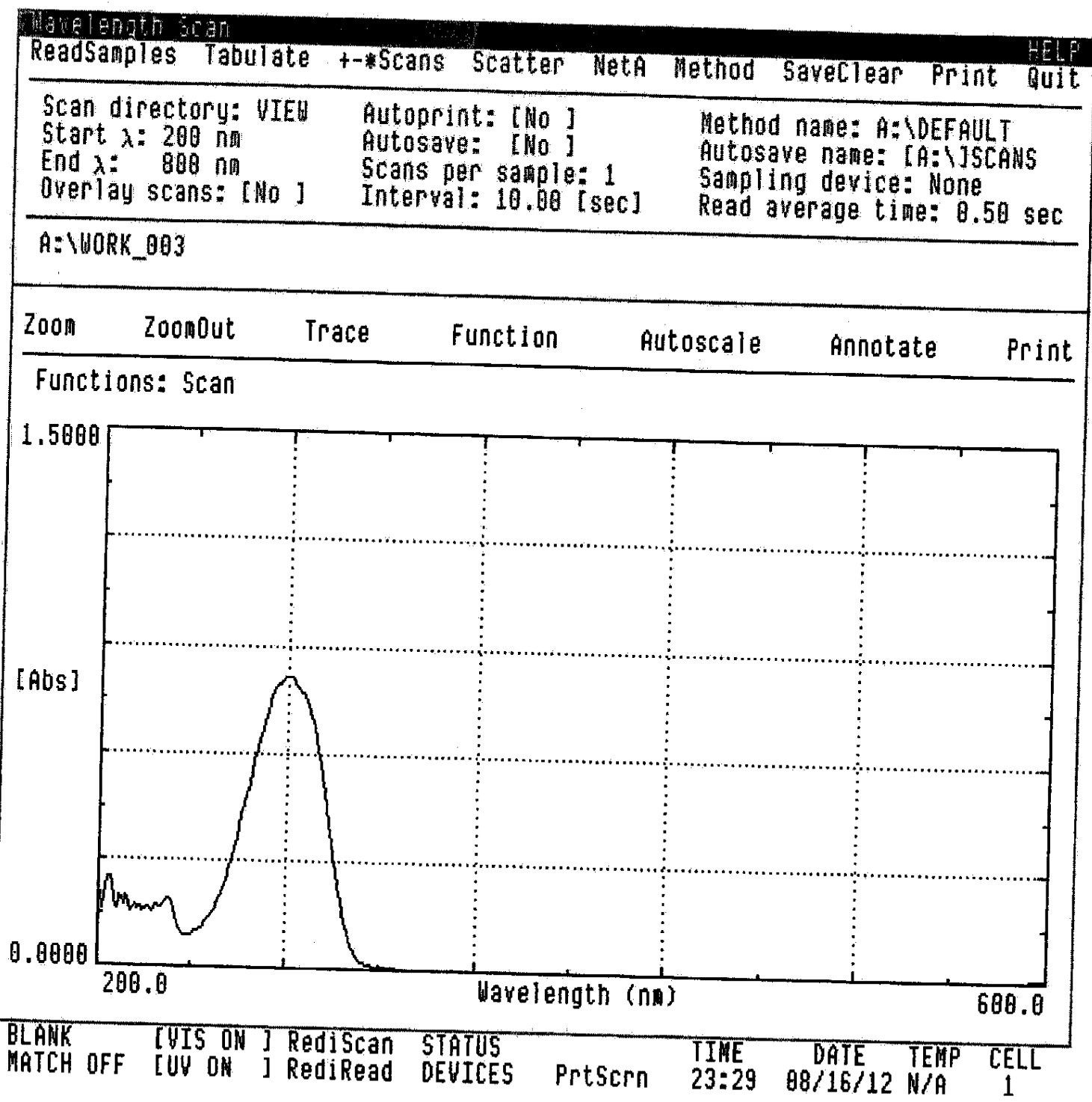


Figure a.2.3 UV-Vis Spectrum for benzocaine.



### **III. Operating Procedures for the Thermo-Scientific 6700 FTIR**

#### To Power on the Instrument:

1. Turn on nitrogen tank and adjust pressure to between 5-10 SCFH air.
2. Open auxiliary nitrogen purge inside sample holding compartment of FTIR.
3. Allow system to nitrogen purge for 20 minutes.

#### Starting OMINC and Instrument Set-Up:

1. Open OMINC from desktop.
2. Click *Expt Set* (Experiment Setup) in top left corner to change/check experiment setting.
3. Align laser under **Experiment – Diagnostics – Align**.
4. Save setting.

#### Running a Sample:

1. Collect Background by clicking **Col Bkg** in top left corner.
2. Insert pellet (KBr or NaCl) into sample holding device and then into FTIR compartment.
3. Collect Sample Spectrum by clicking **Col Smp** in the top left corner.
4. Save raw spectrum to desired location.

#### Analyzing Spectra:

##### *Assigning Peaks:*

Clicking **Find Pks** will automatically assign wave-number of signal peaks. Sensitivity can be adjusted by manipulating the scale on the left while detection height can be adjusted by clicking the spectra.

##### *Library Comparison:*

1. Select **Analyze – Library** setup and then add desired or all libraries to search list
2. To compare, select **Analyze – Search**.

#### Shutting Down FTIR:

1. Close out of OMNIC, log off computer and shut off monitor.
2. Close auxiliary purge inside of sample holding compartment by pushing in on small silver button on the side.
3. Close valve on nitrogen tank.

#### **IV. Operating Procedures for the Beckman DU-7400 Spectrophotometer**

##### To Power on the Instrument:

1. Turn on the Instrument power switch, located at the right rear of the instrument near the bottom. A power-up diagnostics screen will appear.
2. The Power-up Pass screen will appear. Click on QUIT. The main instrument screen will appear.
3. Click on VIS OFF near the bottom left on the screen, it will then read VIS ON in red.
4. Click on UV OFF near the bottom left on the screen, it will then read UV ON in red.
5. Allow the lamp to warm up for 5 minutes.

##### Instrument Set-Up:

1. Click on the WAVELENGTH SCAN option.
2. A blank graph of Absorbance (y-axis) versus Wavelength (x-axis) will appear on the screen. Adjust to desired scale by clicking the x- or y-axis and typing the appropriate number in the calculator pad that appears.

##### Running a Sample:

1. Insert "blank" cuvette containing the pure solvent in the light path (the furthest position in on the track), click on BLANK at the bottom left of screen. A Reading Blank message will appear.
2. When Reading Blank message is gone, remove the "blank" cuvette, and insert your sample cuvette in the same slot in the light path. Click on READ SAMPLES near the top of the screen. Wait until the spectrum has been measured and the resulting graph of absorbance versus wavelength appears.

##### Analyzing Spectra:

1. To assess the lambda max values for the sample, examine the graph by moving a vertical hairline across the spectrum. To do so, click on **Trace**. The hairline will appear on your graph, and an inset box will show the Absorbance reading that corresponds to the particular wavelength where the hairline sits. To move hairline, click the left mouse cursor to move the hairline to the left, and click the right mouse cursor to move the line to the right. Move the hairline across the screen and record the wavelength and the corresponding Absorbance reading at each maximum on the spectrum.
2. Click **PrtScrn** to print graphical results.

##### Shutting Down UV-Vis:

1. Turn lamp off by clicking the red VIS ON and UV ON on the instrument screen.
2. Click on QUIT.